

Generalized Interference of Fermions and Bosons

Dylan Spivak

Department of Mathematical Sciences, Lakehead University, Thunder Bay, Ontario P7B 5E1, Canada

Murphy Yuezhen Niu

Department of Physics, Massachusetts Institute of Technology, Cambridge, Massachusetts 02139, USA

Barry C. Sanders

Institute for Quantum Science and Technology, University of Calgary, Alberta T3A 0E1, Canada

Hubert de Guise

Department of Physics, Lakehead University, Thunder Bay, Ontario P7B 5E1, Canada

Using tools from representation theory, we derive expressions for the coincidence rate of partially-distinguishable particles in an interferometry experiment. Our expressions are valid for either bosons or fermions, and for any number of particles. In an experiment with n particles the expressions we derive contain a term for each partition of the integer n ; Gamas's theorem is used to determine which of these terms are automatically zero based on the pairwise level of distinguishability between particles. Most sampling schemes (such as Boson Sampling) are limited to completely indistinguishable particles; our work aids in the understanding of systems where an arbitrary level of distinguishability is permitted. As an application of our work we introduce a sampling scheme with partially-distinguishable fermions, which we call Generalized Fermion Sampling.

I. INTRODUCTION

In this paper we investigate coincidence rates for n particles arriving not necessarily simultaneously at n detectors located at the output of an $m \times m$ unitary linear interferometer. We extend previous work on coincidence rates [1–5] for partially distinguishable particles, either bosons or fermions; in doing this we improve on the understanding of the Hong-Ou-Mandel effect [6] for many-particle systems [7]. Our work is motivated by the problem of BOSONSAMPLING [8], which has thrown new bridges between computational complexity and linear optics but initially dealt with indistinguishable, simultaneous bosons. The boson-sampling computational challenge is to ascertain, computationally and experimentally, the distribution of coincidence rates as the location of the detectors is changed. The excitement of boson sampling and its associated computational problem is that coincidence rates for indistinguishable bosons are given by permanents [9] of (nearly) Gaussian-random $n \times n$ complex matrices; whereas these permanents are hard to compute, they are easily accessible experimentally [10].

Boson sampling has been generalized to non-simultaneous arrival times [3] and Gaussian states [11]. A more recent refinement of the original boson sampling proposal is the rapidly developing study and implementation of Gaussian BosonSampling [12–16], which leverages the transformation properties of squeezed states to produce an equally hard computational task via computation of a hafnian rather than a permanent. Originally regarded as the quickest way to establish quantum advantage [17], some argue that efficiently solving BOSONSAMPLING could yield a practical benefit [18–22].

Whereas the interference of light is a venerable centuries-old topic [23], fermionic interference is relatively recent, dating back to electron diffraction [24]. The notion of fermion interferometry, as a concept for one or more fermions to face one or more paths, controlled by analogues of beam splitters and phase shifters, extends the concept of fermion interference to controlled interferometric processes [25] such as electronic analogues to Young’s double-slit experiment [26] and fermion antibunching evident in current fluctuations of partitioned electrons [27]. The term fermion interferometry has been used in nuclear physics [28], based on a Hanbury Brown and Twiss type of two-nucleon correlation measurement [29, 30] akin to fermion antibunching [27], and not fermion interferometry as we study here. Some recent advances in the coherent control of electrons, including applications to fermionic interferometry, are reviewed in [31].

It is convenient to think of the permanent, which is often introduced as an “unsigned determinant”, as a group function on a $GL_n(\mathbb{C})$ matrix associated with the fully symmetric representation of the permutation group \mathfrak{S}_n of n objects. From this perspective, the determinant is also a group function but associated with the alternating representation of the permutation group \mathfrak{S}_n .

It is well established that the permanent and the determinant are required to evaluate rates for simultaneous bosons and fermions, respectively. Here, we will show as a first result of this paper that, for nonsimultaneous arrival times, additional group functions beyond the permanent and determinant and associated with other representations of \mathfrak{S}_n , contribute to the coincidence rate. The rate can also be expressed in terms of immanants [32], which generalize matrix determinants and permanents and in fact interpolate between them. A second important result of our work follows as a corollary to Gamas’s theorem [33, 34]: we will show how the mutual partial distinguishability of the particles determines which group functions will have non-zero contributions. To our knowledge, this is the first time Gamas’s theorem has been applied to a physical system. Our third result states that, if at most $\lceil n/2 \rceil$ fermions are indistinguishable, then the exact coincidence rate for fermions contains computationally expensive group functions which require a number of operations that grows exponentially in the number of fermions. As a fourth result, we show that, for uniformly random arrival times, the probability of needing to evaluate these computationally expensive group functions differs from 1 by a quantity that goes to 0 exponentially fast in the number of fermions. This last result naturally leads us to introduce GENFERMIONSAMPLING as the computational problem of sampling the distribution of coincidence rates generated by fermions arriving nonsimultaneously at the detectors.

Before we proceed we need to clarify issues of semantics. By “arrival time”, we are referring to particles whose temporal profile (wave-packet shape) is effectively localized in time; we define the arrival times as the delay between particle creation at the source and the time taken for the wavepacket to travel from the source to the interferometer *output* port. Operationally, our arrival times are effectively controllable delays in the interferometer input channels. If two or more arrival times are the same, the relevant particles “arrive simultaneously” at the detectors; if arrival times are different, the particles are “nonsimultaneous”. Even if the particles do not arrive simultaneously at the detectors, we will speak of coincidence rate in the sense of particles detected during a single run by detectors at selected positions. We imagine an operator triggering the release of particles and opening a detection-time window of some fixed time interval, long enough for particles to arrive at the interferometer, to be scattered in the interferometer and counted at the detectors. The detection-time window then closes and all the detections during this window are described as coincident detections. The rate at which they are detected in coincidence depends on the interferometer, the times of arrival at the interferometer, and positions of the detectors; this rate is called the *coincidence rate* throughout this paper.

II. NOTATION AND MATHEMATICAL PRELIMINARIES

A. The scattering matrix and its submatrices

We envisage an m -channel passive interferometer [35] that receives single particles at n ($n \leq m$) of its input ports and no particles at the rest of the input ports. Mathematically, this interferometer transformation is described by a unitary linear transformation U , which is an $m \times m$ unitary matrix. We assume that U is a Haar-random matrix to avoid any symmetries in the matrix entries that would inadvertently simplify the rate calculations.

For an n -particle input state, with one particle per input port, we label without loss of generality this input by 1 to n as port labels, or, in the Fock basis, as $|1\rangle_n = |1, 1, 1, \dots, 0, 0, 0\rangle$. Detectors are placed at the output ports, and, although either one or zero particles enter each input, more than one particle can be registered at an output detector. For the generic case, we have s_i particles detected at the i^{th} channel, and the total number of particles is conserved such that $\sum_i s_i = n$.

Let $s \in \Phi_{m,n}$, where $\Phi_{m,n}$ is the set of m -tuples (s_1, \dots, s_m) so that $s_1 + \dots + s_m = n$. Mathematically we first construct the $m \times n$ submatrix \mathcal{A} by keeping only the first n columns of U . Next, we construct the $n \times n$ submatrix $A(s)$ for each $s \in \Phi_{m,n}$, by replicating side-by-side s_i times row i of \mathcal{A} , and by deleting all rows for which $s_i = 0$.

In the remainder of this paper we focus on and restrict our presentation and arguments to those strings s with $s_i = 0$ or 1 for all i . Practically, this can be achieved by diluting the particles so that $m \gg n$, in which case the probability that s will contain any $s_i > 1$ is small. Alternatively, one may post-select those events where the above condition holds, ignoring events where some of the $s_i > 1$. As a consequence, all denominator factors of $s_1!s_2!\dots s_m!$ that would appear in a rate are 1, and every submatrix $A(s) \in GL_n(\mathbb{C})$.

B. Enter the permutation group

As mentioned above we envisage a linear lossless interferometer modelled as a unitary $m \times m$ matrix. Suppose that n ($n < m$) particles enter in a subset of the possible input ports, exactly one particle per input port. Without loss of generality we label these input ports from 1 to n . The effect of the interferometer is to scatter each single particle so it eventually reaches one of the detectors; each detector is located at a different output port, and we assume that the n input particles reach n different detectors with exactly one particle per detector. Given a string $s \in \Phi_{m,n}$ so that $s_i = 0$ or 1, the positions of the n detectors registering one particle are now simply the list of those i 's for which $s_i = 1$. This list of detector positions we denote by S , so that S_k is the position of the k^{th} detector that registers a particle. For example, if $s = (0, 1, 1, 0, 1)$, then we have $S = (2, 3, 5)$ with $S_1 = 2, S_2 = 3, S_3 = 5$ as shown in the example of Fig. 1.

Given $s \in \Phi_{m,n}$ and S , the $n \times n$ matrix $A(s)$ thus has elements

$$A(s)_{\beta,\alpha} = U_{S_\beta,\alpha}, \quad \alpha, \beta = 1, \dots, n. \quad (1)$$

With s as above, for instance, we have, using $A(235) := A(01101)$

$$A(235) = \begin{pmatrix} A(235)_{11} & A(235)_{12} & A(235)_{13} \\ A(235)_{21} & A(235)_{22} & A(235)_{23} \\ A(235)_{31} & A(235)_{32} & A(235)_{33} \end{pmatrix} = \begin{pmatrix} U_{21} & U_{22} & U_{23} \\ U_{31} & U_{32} & U_{33} \\ U_{51} & U_{52} & U_{53} \end{pmatrix}. \quad (2)$$

The matrix $A(s)$ is in general not unitary but rather $A(s) \in GL_n(\mathbb{C})$. (Note that, if we allowed more than one particle per output port, $A(s)$ is no longer in $GL_n(\mathbb{C})$.)

During a run of the experiment, the effect of the interferometer is to scatter a single particle state from i to any *one* output port S_k . The data of the n detectors that have registered a particle is then collected. Fig. 1 also shows that particle 1 ends up in detector 2, located at output port 3; particle 2 reaches detector 1 at port 2; and particle 3 reaches detector 3 at port 5. The amplitude for this process is proportional to the monomial $A(s)_{21}A(s)_{12}A(s)_{33}$. There are clearly six possible ways for particles to exit in the three detectors, with exactly one particle per detector, and each of these six possible ways is a permutation of (S_1, S_2, S_3) . The net amplitude is thus a sum of 6 terms of the form $A(s)_{k1}A(s)_{j2}A(s)_{\ell 3}f(\bar{\tau}_1)g(\bar{\tau}_2)h(\bar{\tau}_3)$, where (k, j, ℓ) is a permutation of (S_1, S_2, S_3) and f, g, h are functions of the individual arrival times at the interferometer.

More generally, as we restrict ourselves to situations where the n particles are detected in different output ports, the effect of the interferometer is to shuffle the input $(1, \dots, n)$ so that particles can exit in $n!$ possible ways at the output, with each of these indexed by a permutation of $(1, \dots, n)$. Each of these $n!$ ways is one term to be added to obtain the net scattering amplitude for this fixed set of detector positions. We see that the permutation (or symmetric) group \mathfrak{S}_n [36, 37] of n particles enters into the problem of computing coincidence rates in a natural way.

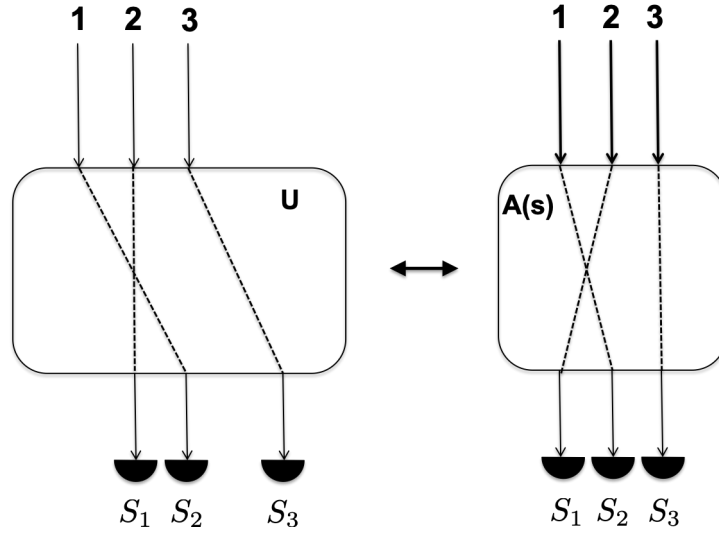


FIG. 1. An example of an interferometer with $m = 5$ and 3 particles, illustrating the labelling and notation for the matrices U and $A(s)$.

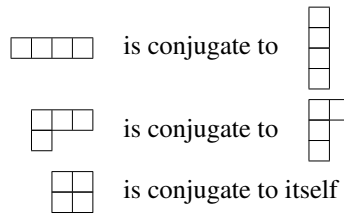
C. Partitions, Immanants, and group functions

Here we explain matrix immanants which - like the permanent or the determinant - are polynomials in the entries of a matrix, albeit neither fully symmetric nor antisymmetric, and are thus naturally well suited to understand the structure of coincidence rates for partially distinguishable particles. Immanants are closely related to Young diagrams, Young tableaux, and general irreducible representations of \mathfrak{S}_n ; the references [38–40] are especially helpful for a longer discussion of these concepts. Additional details on this background can be also found in [41].

The study of the permutation group is closely tied to the partitions of n , as these partitions label the irreducible representations of \mathfrak{S}_n . A partition of a positive integer n is a k -tuple $\lambda = (\lambda_1, \lambda_2, \dots, \lambda_k)$ such that $\lambda_1 \geq \lambda_2 \geq \dots \geq \lambda_k \geq 1$ and $\sum_{i=1}^k \lambda_i = n$; we call k the number of parts of a partition, λ_1 the width, and n the size. The notation $\lambda \vdash n$ means that λ is a partition of n . A Young diagram is a visual way to write a partition using boxes. Given a partition λ , we construct the associated Young diagram by placing a row of λ_1 boxes at the top, then we add a left-justified row of λ_2 boxes is added directly below. This process is repeated for each λ_i . The partition λ is referred to as the shape of the Young diagram.

We also need the partition λ^* conjugate to the partition λ , which is obtained from λ by exchanging rows and columns of λ . This is equivalent to reflecting the diagram λ about the main diagonal.

Example 1: Conjugate partitions for \mathfrak{S}_4 :



A Young tableau (plural tableaux) on a Young diagram of size n is a numbering of the boxes using entries from the set $\{1, 2, \dots, n\}$. A standard tableau has its entries strictly increasing across rows and strictly increasing down the columns, as a result each integer from 1 to n appears exactly once in the tableau. The conditions for the semi-standard tableaux are relaxed: entries weakly increase along rows, but still must increase strictly down columns. We use the notation s_λ and d_λ for the number of standard and semi-standard Young tableaux of shape λ , respectively.

For an arbitrary $n \times n$ matrix B , there is an immanant defined for every partition of n . The λ -immanant of B is

$$\text{imm}^\lambda(B) := \sum_{\sigma \in \mathfrak{S}_n} \chi_\lambda(\sigma) \prod_{i=1}^n B_{\sigma(i), i}. \quad (3)$$

The notation $\chi_\lambda(\sigma)$ refers to the character of element σ in the λ -representation of \mathfrak{S}_n . The permanent and determinant are special cases of immanants that correspond to the trivial representation and the alternating representation, respectively. The

simplest non-trivial example is the \square -immanant of a 3×3 matrix

$$\text{imm}^{\square}(B) = 2B_{11}B_{22}B_{33} - B_{21}B_{32}B_{13} - B_{31}B_{12}B_{23}. \quad (4)$$

Kostant provides a connection between certain group functions of $GL_n(\mathbb{C})$ and immanants [42]. Let $B \in GL_n(\mathbb{C})$ and consider the representation D_λ of $GL_n(\mathbb{C})$, namely,

$$\begin{aligned} D_\lambda : GL_n(\mathbb{C}) &\rightarrow GL_{d_\lambda}(\mathbb{C}) \\ B &\rightarrow D_\lambda(B). \end{aligned} \quad (5)$$

A \mathcal{D} -function is a function of the form

$$\mathcal{D}_{i,j}^\lambda(B) = \langle \psi_i^\lambda | D_\lambda(B) | \psi_j^\lambda \rangle, \quad (6)$$

where $|\psi_i^\lambda\rangle$ is a basis vector of the representation space of the D_λ representation of $GL_n(\mathbb{C})$. Define $\mathcal{D}^\lambda(B)$ to be the matrix with $\mathcal{D}_{i,j}^\lambda(B)$ as its ij^{th} entry. We are particularly interested in the states $|\psi_j^\lambda\rangle$ that live in the $(1, 1, 1, \dots, 1)$ -weight subspace of D_λ (if $B \in SU(n)$ this is referred to as the 0-weight subspace). Recall that a vector $v \in \mathbb{C}^n$ has weight $w = (w_1, w_2, \dots, w_n)$ when

$$\text{diag}(t_1, t_2, \dots, t_n)v = t_1^{w_1} t_2^{w_2} \dots t_n^{w_n} v. \quad (7)$$

The following theorem of Kostant shows a deep relationship between immanants and \mathcal{D} -functions.

Theorem 2: (Kostant [42]): Given $B \in GL_n(\mathbb{C})$, it follows that

$$\text{imm}^\lambda(B) = \sum_i \mathcal{D}_{i,i}^\lambda(B), \quad (8)$$

where the sum is over all states of weight $(1, 1, 1, \dots, 1)$. This connection is important to establish the complexity of evaluating the coincidence rate equations.

III. RATES FOR CONTINUOUS TIME

We analyze coincidence rates of an experiment where n particles are modelled by a Gaussian wave packet arriving in an $m \times m$ interferometer at times $\bar{\tau}_1, \dots, \bar{\tau}_n$, and obtain a compact form for the bosonic and fermionic coincidence rate equations. The difference between the boson and fermion cases is a sign of some entries of an $n! \times n!$ symmetric matrix $R(\bar{\tau}; \mathfrak{p})$ containing information about the level of distinguishability through the arrival times $\bar{\tau}$. The species label \mathfrak{p} can be either \mathfrak{b} for bosons or \mathfrak{f} for fermions. The permutation group \mathfrak{S}_n of n particles is an important tool throughout this discussion. If two or more elements of \mathfrak{S}_n need to be specified, we do so with a subscript v.g. σ_i or γ_j etc.

A. Sources, input state, arrival-time vector, detectors

We model a source for input channel k as producing a temporal Gaussian wave packet in channel k ; the wavepacket is described by the one-particle state

$$|k(\bar{\tau}_k)\rangle := \hat{A}_k^\dagger(\bar{\tau}_k) |0\rangle = \int d\omega_k \phi(\omega_k) e^{-i\omega_k \bar{\tau}_k} \hat{a}_k^\dagger(\omega_k) |0\rangle, \quad (9)$$

where the spectral profile

$$\phi(\omega_k) = \frac{1}{\sqrt{\Delta\omega}\sqrt{2\pi}} e^{-\frac{(\omega_k - \omega_0)^2}{4(\Delta\omega)^2}} \quad (10)$$

is normalized so that $\int d\omega_k |\phi(\omega_k)|^2 = 1$. The frequency spread of the source $\Delta\omega$ is sufficiently narrow and assumed constant, so that one can replace the energy $\hbar\omega$ of each Fourier component by the mean excitation energy of the photon [43]. Here, operators such as $\hat{a}_i^\dagger(\omega_k)$ —they can be either fermionic or bosonic—create an excitation of frequency ω_k in input channel i .

We assume n independent but identical sources, each delivering one wave packet to a separate input channel, with n smaller than or equal to the total number m of channels. Let

$$|0\rangle = |0\rangle_1 \otimes |0\rangle_2 \otimes |0\rangle_3 \otimes \cdots \otimes |0\rangle_n, \quad (11)$$

denote the n -particle vacuum state; the n -particle input state is then the n -fold product state [43]

$$|\psi_{in}(\bar{\tau}_1, \dots, \bar{\tau}_n)\rangle := \hat{A}_1^\dagger(\bar{\tau}_1)\hat{A}_2^\dagger(\bar{\tau}_2)\dots\hat{A}_n^\dagger(\bar{\tau}_n)|0\rangle. \quad (12)$$

The times of arrival

$$\bar{\tau} := [\bar{\tau}_1, \dots, \bar{\tau}_n] \quad (13)$$

that appear in Eq. (12) are continuous real numbers in some finite time interval of duration \mathcal{T} and are measured from some common but otherwise arbitrary reference time. The detectors are Fourier-limited [44]. They integrate with frequency response $\Phi(\Delta\Omega)$ over the entire interval \mathcal{T} so that long integration times lead to small width $\Delta\Omega$; they are modelled as projection operators

$$\hat{\Pi}_k = \int d\Omega_k \hat{a}_k^\dagger(\Omega_k) |0\rangle \langle 0| \hat{a}_k(\Omega_k) \Phi(\Delta\Omega_k), \quad (14)$$

$$\hat{\Pi} = \hat{\Pi}_1 \otimes \hat{\Pi}_2 \otimes \cdots \otimes \hat{\Pi}_n. \quad (15)$$

For simplicity we choose the frequency response of all detectors to be identical Gaussians of the form

$$\Phi(\Delta\Omega) = \frac{1}{\Delta\Omega\sqrt{2\pi}} e^{-\frac{(\Omega-\omega_0)^2}{2(\Delta\Omega)^2}} \quad (16)$$

with fixed width $\Delta\Omega$. A detector does not register arrival times, but registers only if a particle has entered the detector at any time during one run of the experiment. The probability of detection at a particular detector depends on $\bar{\tau}$ and on the submatrix $A(s)$.

B. Exact coincidence rate equations, continuous time

In this subsection, we obtain a compact form for the bosonic and fermionic coincidence rate equations, and show how they are closely related. We also show that the entries of an $n! \times n!$ symmetric matrix $R(\bar{\tau}; \mathbf{p})$ are monomials in the entries of the so-called delay matrix $r(\bar{\tau})$, defined in Eq. (29). This observation is crucial to our simplifications. In §IV, we use Gammas's theorem to deduce the conditions under which the λ -immanant of $r(\bar{\tau})$ is zero based on the set of arrival times $\bar{\tau}$.

The effect of the interferometer is to scatter each single particle state to

$$|k(\bar{\tau}_i)\rangle \rightarrow A(s) |k(\bar{\tau}_i)\rangle = \sum_q |q(\bar{\tau}_i)\rangle A(s)_{qk}, \quad (17)$$

i.e. the scattering matrix produces superposition of states from the initial state but does not affect the times of arrival. The scattered state can be written in expanded form as

$$\begin{aligned} |\text{out}(\bar{\tau})\rangle &= \sum_{\sigma \in \mathfrak{S}_n} A(s)_{\sigma(1)1} A(s)_{\sigma(2)2} \cdots A(s)_{\sigma(n)n} \\ &\times \int d\omega_1 d\omega_2 \cdots d\omega_n \phi(\omega_1) \phi(\omega_2) \cdots \phi(\omega_n) e^{-i\omega_1 \bar{\tau}_1} e^{-i\omega_2 \bar{\tau}_2} \cdots e^{-i\omega_n \bar{\tau}_n} \\ &\times \hat{a}_{\sigma(1)}^\dagger(\omega_1) \hat{a}_{\sigma(2)}^\dagger(\omega_2) \cdots \hat{a}_{\sigma(n)}^\dagger(\omega_n) |0\rangle. \end{aligned} \quad (18)$$

To simplify the expressions for the rates, choose some ordering for the elements γ_i of \mathfrak{S}_n and introduce the following shorthand notation for monomials. Let M be some $n \times n$ matrix, and write for the product

$$M_{\gamma(1),1} M_{\gamma(2),2} \cdots M_{\gamma(n),n} := \mathbf{M}_\gamma. \quad (19)$$

To highlight and contrast the boson and fermion cases, we treat them in quick succession. In the bosonic case, the evaluation of the coincidence rate

$$\text{rate}(\bar{\tau}, s; \mathbf{b}) := \langle \text{out} | \hat{\Pi} | \text{out} \rangle, \quad (20)$$

is best understood when written in the form

$$\langle \text{out} | \hat{\Pi} | \text{out} \rangle = \mathcal{N}^{n!} \sum_{\sigma, \gamma \in \mathfrak{S}_n} \mathbf{A}(s)_\gamma^* [R(\bar{\tau}; \mathbf{b})]_{\gamma, \sigma} \mathbf{A}(s)_\sigma, \quad (21)$$

$$\mathcal{N} = \frac{1}{\sqrt{2\pi(\Delta\omega^2 + \Delta\Omega^2)}}, \quad (22)$$

where \mathcal{N} is a normalization factor, $\mathbf{A}(s)_\sigma$ is the monomial defined in Eq. (19), and where the entries of the $n! \times n!$ matrix $R(\bar{\tau}; \mathbf{b})$ (which we call the (bosonic) rate matrix) are evaluated by taking the operators $\hat{a}_k^\dagger(\omega_j)$ and $\hat{a}_i(\omega_\ell)$ to satisfy the usual boson commutation relations. Evaluation of the element (γ, σ) of the matrix $R(\bar{\tau}; \mathbf{b})$ yields

$$[R(\bar{\tau}; \mathbf{b})]_{\gamma, \sigma} = \exp\left(-\frac{\delta\omega^2(\bar{\tau}_{\gamma^{-1}(1)} - \bar{\tau}_{\sigma^{-1}(1)})^2}{2}\right) \exp\left(-\frac{\delta\omega^2(\bar{\tau}_{\gamma^{-1}(2)} - \bar{\tau}_{\sigma^{-1}(2)})^2}{2}\right) \\ \times \cdots \times \exp\left(-\frac{\delta\omega^2(\bar{\tau}_{\gamma^{-1}(n)} - \bar{\tau}_{\sigma^{-1}(n)})^2}{2}\right), \quad (23)$$

$$\frac{1}{\delta\omega^2} = \frac{1}{\Delta\Omega^2} + \frac{1}{\Delta\omega^2}. \quad (24)$$

For fermions the operators $\hat{a}_k^\dagger(\omega_j)$ and $\hat{a}_i(\omega_\ell)$ satisfy anticommutation relations so an additional negative sign, which comes from an odd number of permutations of fermionic operators, multiplies the $[R(\bar{\tau}; \mathbf{b})]_{\gamma, \sigma}$ term when the permutation $\sigma\gamma$ is odd.

Ignoring the unimportant normalization constant \mathcal{N} for convenience, the coincidence rate is expressed as

$$\text{rate}(\bar{\tau}, s; \mathbf{f}) = \sum_{\sigma, \gamma \in \mathfrak{S}_n} \mathbf{A}(s)_\gamma^* [R(\bar{\tau}; \mathbf{f})]_{\gamma, \sigma} \mathbf{A}(s)_\sigma \quad (25)$$

$$[R(\bar{\tau}; \mathbf{f})]_{\gamma, \sigma} = \text{sgn}(\sigma\gamma) [R(\bar{\tau}; \mathbf{b})]_{\gamma, \sigma} = \chi^{(1^n)}(\sigma\gamma) [R(\bar{\tau}; \mathbf{b})]_{\gamma, \sigma} \quad (26)$$

where $\chi^{(1^n)}(\sigma\gamma)$ is the character of element $\sigma\gamma$ in the one-dimensional fully-antisymmetric (alternating) representation of \mathfrak{S}_n . Eq. (26) shows explicitly how a sign difference between the fermion and boson case can arise.

We next analyze the rate matrices $R(\bar{\tau}; \mathbf{b})$ and $R(\bar{\tau}; \mathbf{f})$ by introducing the delay matrix $r(\bar{\tau})$, which is an $n \times n$ symmetric matrix that keeps track of the relative overlaps between pulses. The (i, j) th entry of $r(\bar{\tau})$ is

$$r_{ij} := e^{\frac{-\delta\omega^2(\bar{\tau}_i - \bar{\tau}_j)^2}{2}}, \quad (27)$$

The entries of this matrix are bounded from 0 to 1, and depend on the level of distinguishability between the particles. In particular, $r_{ij} = 1$ when the arrival times $\tau_i = \tau_j$.

We observe that the delay matrix $r(\bar{\tau})$ is in fact a Gram matrix by considering the basis functions

$$f_k(\omega; \bar{\tau}_k) = e^{-i(\omega - \omega_0)\bar{\tau}_k}, \quad k = 1, 2, \dots, n \quad (28)$$

with the symmetric inner product

$$r_{ij}(\bar{\tau}) = \langle f_i | f_j \rangle = \frac{1}{\mathcal{N}} \int d\omega |\phi(\omega)|^2 \Phi(\Delta\omega) f_i^*(\omega; \bar{\tau}_i) f_j(\omega; \bar{\tau}_j), \quad (29)$$

with ϕ and Φ respectively given in Eqs. (10) and (16). Using the same shorthand notation for the monomials in r as done in Eq. (19), we find that the i th entry of the bosonic rate matrix $R(\bar{\tau}; \mathbf{b})$ is

$$R(\bar{\tau}; \mathbf{b})_{ij} := \mathbf{r}_{\gamma_j^{-1} \eta}(\bar{\tau}) = r_{\gamma_j^{-1} \eta(1), 1}(\bar{\tau}) r_{\gamma_j^{-1} \eta(2), 2}(\bar{\tau}) \cdots r_{\gamma_j^{-1} \eta(n), n}(\bar{\tau}). \quad (30)$$

In the fermionic case, the (i, j) th entry of the rate matrix is

$$R(\bar{\tau}; \mathbf{f})_{ij} = \text{sgn}(\gamma_i \gamma_j) \mathbf{r}_{\gamma_j^{-1} \eta}(\bar{\tau}). \quad (31)$$

For some fixed ordering $\{\gamma_1, \gamma_2, \dots, \gamma_{n!}\}$ of the elements of \mathfrak{S}_n , we conveniently introduce the vector $v(s)$

$$v(s) = (\mathbf{A}(s)_{\gamma_1}, \mathbf{A}(s)_{\gamma_2}, \dots, \mathbf{A}(s)_{\gamma_{n!}})^\top. \quad (32)$$

Eqs. (21) and (25) can respectively be expressed as

$$\text{rate}(\bar{\tau}, s; \mathbf{b}) = \sum_{\sigma, \gamma \in \mathfrak{S}_n} \mathbf{A}(s)_{\gamma}^* \mathbf{r}_{\gamma^{-1}\sigma}(\bar{\tau}) \mathbf{A}(s)_{\sigma}, \quad (33)$$

$$= v^\dagger(s) R(\bar{\tau}; \mathbf{b}) v(s), \quad (34)$$

and

$$\text{rate}(\bar{\tau}, s; \mathbf{f}) = \sum_{\sigma, \gamma \in \mathfrak{S}_n} \text{sgn}(\gamma\sigma) \mathbf{A}(s)_{\gamma}^* \mathbf{r}_{\gamma^{-1}\sigma}(\bar{\tau}) \mathbf{A}(s)_{\sigma}, \quad (35)$$

$$= v^\dagger(s) R(\bar{\tau}; \mathbf{f}) v(s). \quad (36)$$

We will refer to Eqs. (34) and (36) as the coincidence rate equations for bosons and fermions, respectively.

Consider for instance the case $n = 3$. The scattering matrix A (dropping s for the moment to avoid clutter) is

$$A = \begin{pmatrix} A_{11} & A_{12} & A_{13} \\ A_{21} & A_{22} & A_{23} \\ A_{31} & A_{32} & A_{33} \end{pmatrix}. \quad (37)$$

We choose the ordering of \mathfrak{S}_3 elements

$$\{e, (12), (13), (23), (123), (132)\} \quad (38)$$

and the vector $v(s)$ takes the form

$$\begin{aligned} v(s) &= \left(A_{11}A_{22}A_{33}, A_{21}A_{12}A_{33}, A_{31}A_{22}A_{13}, A_{11}A_{32}A_{23}, A_{21}A_{32}A_{13}, A_{31}A_{12}A_{23} \right)^\top, \\ &= (\mathbf{A}_e, \mathbf{A}_{(12)}, \mathbf{A}_{(13)}, \mathbf{A}_{(23)}, \mathbf{A}_{(123)}, \mathbf{A}_{(132)})^\top. \end{aligned} \quad (39)$$

with s implied in the argument of each A_{ij} .

The bosonic rate matrix $R(\bar{\tau}; \mathbf{b})$ takes the form of a Schur power matrix [45]:

$$R(\bar{\tau}; \mathbf{b}) = \begin{pmatrix} \mathbf{r}_e & \mathbf{r}_{(12)} & \mathbf{r}_{(13)} & \mathbf{r}_{(23)} & \mathbf{r}_{(123)} & \mathbf{r}_{(132)} \\ \mathbf{r}_{(12)} & \mathbf{r}_e & \mathbf{r}_{(132)} & \mathbf{r}_{(123)} & \mathbf{r}_{(23)} & \mathbf{r}_{(13)} \\ \mathbf{r}_{(13)} & \mathbf{r}_{(123)} & \mathbf{r}_e & \mathbf{r}_{(132)} & \mathbf{r}_{(12)} & \mathbf{r}_{(23)} \\ \mathbf{r}_{(23)} & \mathbf{r}_{(132)} & \mathbf{r}_{(123)} & \mathbf{r}_e & \mathbf{r}_{(13)} & \mathbf{r}_{(12)} \\ \mathbf{r}_{(132)} & \mathbf{r}_{(23)} & \mathbf{r}_{(12)} & \mathbf{r}_{(13)} & \mathbf{r}_e & \mathbf{r}_{(123)} \\ \mathbf{r}_{(123)} & \mathbf{r}_{(13)} & \mathbf{r}_{(23)} & \mathbf{r}_{(12)} & \mathbf{r}_{(132)} & \mathbf{r}_e \end{pmatrix}, \quad (40)$$

with the arrival-time vector $\bar{\tau}$ implicit in \mathbf{r} . For the fermionic case, we add a negative sign to the entries when $\gamma\gamma_j$ is an odd permutation; the result is

$$R(\bar{\tau}; \mathbf{f}) = \begin{pmatrix} \mathbf{r}_e & -\mathbf{r}_{(12)} & -\mathbf{r}_{(13)} & -\mathbf{r}_{(23)} & \mathbf{r}_{(123)} & \mathbf{r}_{(132)} \\ -\mathbf{r}_{(12)} & \mathbf{r}_e & \mathbf{r}_{(132)} & \mathbf{r}_{(123)} & -\mathbf{r}_{(23)} & -\mathbf{r}_{(13)} \\ -\mathbf{r}_{(13)} & \mathbf{r}_{(123)} & \mathbf{r}_e & \mathbf{r}_{(132)} & -\mathbf{r}_{(12)} & -\mathbf{r}_{(23)} \\ -\mathbf{r}_{(23)} & \mathbf{r}_{(132)} & \mathbf{r}_{(123)} & \mathbf{r}_e & -\mathbf{r}_{(13)} & -\mathbf{r}_{(12)} \\ \mathbf{r}_{(132)} & -\mathbf{r}_{(23)} & -\mathbf{r}_{(12)} & -\mathbf{r}_{(13)} & \mathbf{r}_e & \mathbf{r}_{(123)} \\ \mathbf{r}_{(123)} & -\mathbf{r}_{(13)} & -\mathbf{r}_{(23)} & -\mathbf{r}_{(12)} & \mathbf{r}_{(132)} & \mathbf{r}_e \end{pmatrix}. \quad (41)$$

Note that, as $r_{ij}(\bar{\tau}) = r_{ji}(\bar{\tau})$, for any permutation σ we have that $\mathbf{r}_\sigma(\bar{\tau}) = \mathbf{r}_{\sigma^{-1}}(\bar{\tau})$, which in turn means that the rate matrix is symmetric with $r_{ii} = 1$. In Table I each of the $\mathbf{r}_\sigma(\bar{\tau})$ terms is expressed as a monomial in the entries of the delay matrix.

The expression of Eq. (34) clearly shows that, in general, the exact expression for the rate involves the multiplication of $1 \times n! \times n! \times n! \times n! \times 1$ quantities. Our job is to cut down on this in two steps. Anticipating results of §IV, we make the crucial observation that, if none of the r_{ij} terms are 0, every permutation occurs exactly once in each row and each column of the rate matrix $R(\bar{\tau}; \mathbf{p})$, hence $R(\bar{\tau}; \mathbf{p})$ carries the regular representation ρ_{reg} of the permutation group. (Although we are here working under the assumption that $s_i = 0$ or 1, this observation on the structure of the rate matrix holds even if some $s_i > 1$.) It is well known that in the decomposition of the regular representation, each irrep of \mathfrak{S}_n appears as many times as its dimension

$$\rho_{\text{reg}} = \bigoplus_{\lambda \vdash n} \bigoplus_{s_\lambda} \rho_\lambda. \quad (42)$$

\mathbf{r}_σ	Monomial in r_{ij} entries	Simplified Monomial
\mathbf{r}_e	$r_{11}r_{22}r_{33}$	1
$\mathbf{r}_{(12)}$	$r_{21}r_{12}r_{33}$	r_{12}^2
$\mathbf{r}_{(13)}$	$r_{31}r_{22}r_{13}$	r_{13}^2
$\mathbf{r}_{(23)}$	$r_{11}r_{32}r_{23}$	r_{23}^2
$\mathbf{r}_{(123)}$	$r_{21}r_{32}r_{13}$	$r_{12}r_{23}r_{13}$
$\mathbf{r}_{(132)}$	$r_{31}r_{12}r_{23}$	$r_{12}r_{23}r_{13}$

TABLE I. Entries of the coincidence rate matrices. The arrive-time vector $\bar{\tau}$ is implicit.

It follows there exists a linear transformation T , determined by the representation theory of \mathfrak{S}_n , that brings the rate matrix to its block diagonal form. In §IV B, we use this property to simplify the coincidence rate equations. Secondly, we show in §V that, for a given set of arrival times $\bar{\tau}$, certain blocks of the diagonalized rate matrix are automatically zero as a consequence of Gammas's theorem.

IV. BLOCK DIAGONALIZATION AND CONTINUOUS TIME

We proceed by leveraging the permutation symmetries of the matrix $R(\bar{\tau}; \mathbf{p})$ and decompose this matrix into irreps of \mathfrak{S}_n , *i.e.* we now show how it is possible to transform the expression of the coincidence rate equations to one where the rate matrix $R(\bar{\tau}; \mathbf{b})$ or $R(\bar{\tau}; \mathbf{f})$ has a block-diagonal form. These symmetries in turn stem from the structure of the matrix $r(\bar{\tau})$. We assume in §IV A, §IV B and §IV C, that for particles i and j with $i \neq j$, no $r_{ij} = 0$, *i.e.* no particle is fully distinguishable from any of the others. When some $r_{ij} = 0$, the matrix $R(\bar{\tau}; \mathbf{f})$ will have 0's and may carry representations of \mathfrak{S}_{n-p} , so the problem is effectively one of $n-p$ partially distinguishable particles. We will discuss the case where some of the particles are fully distinguishable from others in §IV D.

An essential point is that, when all $r_{ij} \neq 0$, the block-diagonalization procedure is independent of the arrival times and independent of the numerical values of entries in the submatrix $A(s)$: it depends *only* on the action of the permutation group \mathfrak{S}_n on monomials $\mathbf{A}(s)_\gamma$ and $\mathbf{r}_\sigma(\bar{\tau})$.

A. Schur-Weyl duality and the decomposition of $\otimes^n \mathbb{C}^n$

We first show that for any string s with $s_i = 0$ or 1, an input state of the type Eq. (12) can be decomposed into pieces which transform nicely under the action of the permutation group. For fixed $\bar{\tau}$, the states $\{\hat{A}_j^\dagger(\bar{\tau})|0\rangle, j = 1, \dots, n\}$ form a basis in \mathbb{C}^n for the n -dimensional defining representation of $GL_n(\mathbb{C})$:

$$\hat{A}_1^\dagger(\bar{\tau})|0\rangle \rightarrow \begin{pmatrix} 1 \\ 0 \\ \vdots \\ 0 \end{pmatrix}, \quad \hat{A}_2^\dagger(\bar{\tau})|0\rangle \rightarrow \begin{pmatrix} 0 \\ 1 \\ \vdots \\ 0 \end{pmatrix}, \quad \dots \quad \hat{A}_n^\dagger(\bar{\tau})|0\rangle \rightarrow \begin{pmatrix} 0 \\ 0 \\ \vdots \\ 1 \end{pmatrix}. \quad (43)$$

Clearly $\hat{A}_j^\dagger(\bar{\tau})|0\rangle$ has weight $(0, 0, \dots, 1_j, \dots, 0)$, with 0 everywhere except 1 in the j^{th} entry. Thus, the product state of Eq. (12) is a state of weight $(1, 1, \dots, 1)$ in the n -fold tensor product of defining representation of $GL_n(\mathbb{C})$. Scattering by a $GL_n(\mathbb{C})$ matrix and subsequent arrivals at different detectors map this product state to a linear combination of states in the same space of states with weight $(1, 1, \dots, 1)$.

Now, it is well known that this n -fold tensor product decomposes as

$$\otimes^n \mathbb{C}^n = \sum_{\lambda \vdash n} \rho_\lambda \otimes D_\lambda \quad (44)$$

where ρ_λ and D_λ are irreducible representations of \mathfrak{S}_n and $GL_n(\mathbb{C})$, respectively. For economy we henceforth write the partition λ for the irrep ρ_λ of \mathfrak{S}_n . When restricted to the $(1, 1, \dots, 1)$ subspace, the n -fold product $\otimes^n \mathbb{C}^n$ is a carrier space for the regular representation of \mathfrak{S}_n [46]. In other words, it is possible to decompose the input and output states into linear combinations of states that transform irreducibly under $\mathfrak{S}_n \otimes GL_n(\mathbb{C})$.

B. Block diagonalization of the coincidence rate equations

Since the rate matrix carries the regular representation of \mathfrak{S}_n , there exists a linear transformation T that block diagonalizes it:

$$\begin{aligned} \text{rate}(\boldsymbol{\tau}, s; \mathbf{p}) &= \mathbf{v}^\dagger(s) R(\boldsymbol{\tau}; \mathbf{p}) \mathbf{v}(s) \\ &= \mathbf{v}^\dagger(s) T^{-1} (TR(\boldsymbol{\tau}; \mathbf{p})) T^{-1} T \mathbf{v}(s) \\ &= (T \mathbf{v}(s))^\dagger (TR(\boldsymbol{\tau}; \mathbf{p}) T^{-1}) (T \mathbf{v}(s)), \end{aligned} \quad (45)$$

where the species label \mathbf{p} stands for either boson (b) or fermion (f).

Fraktur letters are used to shorten notation:

$$\mathbf{v}(s) = T \mathbf{v}(s) \quad \text{and} \quad \mathfrak{R}(\boldsymbol{\tau}; \mathbf{p}) \equiv TR(\boldsymbol{\tau}; \mathbf{p}) T^{-1}. \quad (46)$$

We write $\mathfrak{R}^\lambda(\boldsymbol{\tau})$ to denote the block that corresponds to irrep λ which appears s_λ times in the block diagonalization. The set of matrices $\mathfrak{R}^\lambda(\boldsymbol{\tau})$ are the same for both bosons and fermions; however, their placement in the block-diagonalized rate matrix $\mathfrak{R}(\boldsymbol{\tau}; \mathbf{p})$ depends on the species label \mathbf{p} and the choice of linear transformation T .

In the bosonic case, when the multiplication $\mathfrak{R}(\boldsymbol{\tau}; \mathbf{b}) \mathbf{v}(s)$ is preformed, the i^{th} copy of the matrix $\mathfrak{R}^\lambda(\boldsymbol{\tau})$ sees s_λ entries of the vector $\mathbf{v}(s)$; we take these entries and construct the vector $\mathbf{v}_{\lambda;i}(s)$. The notation $\mathbf{v}_{\lambda;i}^j(s)$ refers to the j^{th} entry of the vector $\mathbf{v}_{\lambda;i}(s)$. The rate is then written as

$$\begin{aligned} \text{rate}(\boldsymbol{\tau}, s; \mathbf{b}) &= \mathbf{v}^\dagger(s) \mathfrak{R}(\boldsymbol{\tau}; \mathbf{b}) \mathbf{v}(s) \\ &= \begin{bmatrix} \mathbf{v}_{\square\square;1}(s) \\ \mathbf{v}_{\square;1}(s) \\ \mathbf{v}_{\square;1}^1(s) \\ \mathbf{v}_{\square;1}^2(s) \\ \mathbf{v}_{\square;2}^1(s) \\ \mathbf{v}_{\square;2}^2(s) \end{bmatrix}^\dagger \begin{bmatrix} \mathfrak{R}^{\square\square}(\boldsymbol{\tau}) & 0 & 0 & 0 & 0 & 0 \\ 0 & \mathfrak{R}^{\square}(\boldsymbol{\tau}) & 0 & 0 & 0 & 0 \\ 0 & 0 & \mathfrak{R}_{1,1}^{\square}(\boldsymbol{\tau}) & \mathfrak{R}_{1,2}^{\square}(\boldsymbol{\tau}) & 0 & 0 \\ 0 & 0 & \mathfrak{R}_{2,1}^{\square}(\boldsymbol{\tau}) & \mathfrak{R}_{2,2}^{\square}(\boldsymbol{\tau}) & 0 & 0 \\ 0 & 0 & 0 & 0 & \mathfrak{R}_{1,1}^{\square}(\boldsymbol{\tau}) & \mathfrak{R}_{1,2}^{\square}(\boldsymbol{\tau}) \\ 0 & 0 & 0 & 0 & \mathfrak{R}_{2,1}^{\square}(\boldsymbol{\tau}) & \mathfrak{R}_{2,2}^{\square}(\boldsymbol{\tau}) \end{bmatrix} \begin{bmatrix} \mathbf{v}_{\square\square;1}(s) \\ \mathbf{v}_{\square;1}(s) \\ \mathbf{v}_{\square;1}^1(s) \\ \mathbf{v}_{\square;1}^2(s) \\ \mathbf{v}_{\square;2}^1(s) \\ \mathbf{v}_{\square;2}^2(s) \end{bmatrix} \end{aligned} \quad (47)$$

The fermion case has one key difference from the boson case. Recall that characters of conjugate representations of \mathfrak{S}_n only differ by a sign in their odd permutations, and that the bosonic and fermionic rate matrices have this symmetry. As a result when the fermionic rate matrix is block-diagonalized into irreducible representations by T , *every matrix representation \mathfrak{R}^λ that appears in the block-diagonalization for boson is replaced by its conjugate \mathfrak{R}^{λ^*} for fermions*. Thus, the coincidence rate equations for the 3-fermion case has the blocks $\mathfrak{R}^{\square}(\boldsymbol{\tau})$ and $\mathfrak{R}^{\square\square}(\boldsymbol{\tau})$ interchanged:

$$\begin{aligned} \text{rate}(\boldsymbol{\tau}, s; \mathbf{f}) &= \mathbf{v}^\dagger(s) \mathfrak{R}(\boldsymbol{\tau}; \mathbf{f}) \mathbf{v}(s) \\ &= \begin{bmatrix} \mathbf{v}_{\square\square;1}(s) \\ \mathbf{v}_{\square;1}(s) \\ \mathbf{v}_{\square;1}^1(s) \\ \mathbf{v}_{\square;1}^2(s) \\ \mathbf{v}_{\square;2}^1(s) \\ \mathbf{v}_{\square;2}^2(s) \end{bmatrix}^\dagger \begin{bmatrix} \mathfrak{R}^{\square}(\boldsymbol{\tau}) & 0 & 0 & 0 & 0 & 0 \\ 0 & \mathfrak{R}^{\square\square}(\boldsymbol{\tau}) & 0 & 0 & 0 & 0 \\ 0 & 0 & \mathfrak{R}_{1,1}^{\square}(\boldsymbol{\tau}) & \mathfrak{R}_{1,2}^{\square}(\boldsymbol{\tau}) & 0 & 0 \\ 0 & 0 & \mathfrak{R}_{2,1}^{\square}(\boldsymbol{\tau}) & \mathfrak{R}_{2,2}^{\square}(\boldsymbol{\tau}) & 0 & 0 \\ 0 & 0 & 0 & 0 & \mathfrak{R}_{1,1}^{\square}(\boldsymbol{\tau}) & \mathfrak{R}_{1,2}^{\square}(\boldsymbol{\tau}) \\ 0 & 0 & 0 & 0 & \mathfrak{R}_{2,1}^{\square}(\boldsymbol{\tau}) & \mathfrak{R}_{2,2}^{\square}(\boldsymbol{\tau}) \end{bmatrix} \begin{bmatrix} \mathbf{v}_{\square\square;1}(s) \\ \mathbf{v}_{\square;1}(s) \\ \mathbf{v}_{\square;1}^1(s) \\ \mathbf{v}_{\square;1}^2(s) \\ \mathbf{v}_{\square;2}^1(s) \\ \mathbf{v}_{\square;2}^2(s) \end{bmatrix}. \end{aligned} \quad (48)$$

When each $s_i = 1$ or 0 , the $\mathbf{v}_{\lambda,i}(s)$ are group functions of weight $(1, 1, 1, \dots, 1)$ for the irrep λ . Thus for any value of n , the

respective coincidence rate equations for bosons and fermions take the general form:

$$\text{rate}(\bar{\tau}, s; \text{b}) = \sum_{\lambda \vdash n} \sum_{i=1}^{s_\lambda} v_{\lambda,i}^\dagger(s) \mathfrak{R}^\lambda(\bar{\tau}) v_{\lambda,i}(s), \quad (49)$$

$$= |\text{per}(A(s))|^2 \text{per}(r(\bar{\tau})) + [\text{other } \mathfrak{S}_n \text{ irreps}] + |\det(A(s))|^2 \det(r(\bar{\tau})),$$

$$\text{rate}(\bar{\tau}, s; \text{f}) = \sum_{\lambda \vdash n} \sum_{i=1}^{s_\lambda} v_{\lambda,i}^\dagger(s) \mathfrak{R}^{\lambda^*}(\bar{\tau}) v_{\lambda,i}(s), \quad (50)$$

$$= |\det(A(s))|^2 \text{per}(r(\bar{\tau})) + [\text{other } \mathfrak{S}_n \text{ irreps}] + |\text{per}(A(s))|^2 \det(r(\bar{\tau})).$$

The notation $\lambda \vdash n$ means that we sum over all partitions of n , and λ^* is the conjugate partition of λ . In particular, when all relative arrival times are identical, *i.e.* when all particles are exactly indistinguishable, $\text{per}(r(\bar{\tau})) = n!$ and all other terms in the sums of Eqs. (49) and (50) are 0; in the case of bosons, Eq. (49) is then truncated to the modulus square of the permanent of $A(s)$, and we recover the original BOSONSAMPLING result; in the fermion case, only $|\det(A(s))|^2$ survives.

C. Immanants and \mathcal{D} -functions for $\mathfrak{R}^\lambda(\bar{\tau})$ and v_λ

In this subsection we again assume s so that $s_i = 0$ or 1. The result holds for any such s and the string label s is implicit throughout. We show that every entry of the matrix $\mathfrak{R}^\lambda(\bar{\tau})$ is a linear combination of permuted λ -immanants of the delay matrix $r(\bar{\tau})$; and each $v_{\lambda,i}$ is a vector where each entry is a linear combination of permuted λ -immanants of the scattering matrix $A \in GL_n(\mathbb{C})$. The elements of the matrix $\mathfrak{R}^\lambda(\bar{\tau})$ and the vector v are also $GL_n(\mathbb{C})$ group functions, also referred to in the physics literature as Wigner \mathcal{D} -functions [47–49].

Let $\{|\psi_i^\lambda\rangle, i = 1, \dots, s_\lambda\}$ denote the set of $(1, 1, \dots, 1)$ basis states in the $GL_n(\mathbb{C})$ irrep λ . For $g \in GL_n(\mathbb{C})$ the overlap of Eq. (6) specializes to

$$\mathcal{D}_{ij}^\lambda(g) := \langle \psi_i^\lambda | D_\lambda(g) | \psi_j^\lambda \rangle \quad (51)$$

where $D_\lambda(g)$ is the representation of g by the matrix D_λ in the irrep λ .

Example 3: For an arbitrary matrix $Z \in GL_3(\mathbb{C})$, the \mathcal{D}_{ij} functions are given in Table II where:

$$\left| \begin{array}{ccc} 3 & 0 & 0 \\ & 2 & 0 \\ & & 1 \end{array} \right\rangle \rightarrow |\psi_1^{\square\square}\rangle, \quad (52)$$

$$\left| \begin{array}{ccc} 2 & 1 & 0 \\ & 2 & 0 \\ & & 1 \end{array} \right\rangle \rightarrow |\psi_1^{\square\Box}\rangle \quad \left| \begin{array}{ccc} 2 & 1 & 0 \\ & 1 & 1 \\ & & 1 \end{array} \right\rangle \rightarrow |\psi_2^{\square\Box}\rangle, \quad (53)$$

$$\left| \begin{array}{ccc} 1 & 1 & 1 \\ & 1 & 1 \\ & & 1 \end{array} \right\rangle \rightarrow |\psi_1^{\square\Box\Box}\rangle. \quad (54)$$

are the Gelfand-Tsetlin patterns [50–52] for the $(1, 1, 1)$ -states in the $\square\square$, $\square\Box$, and $\square\Box\Box$ subspaces, respectively.

We use Theorem 2 to prove two results about \mathcal{D} -functions. Firstly:

Lemma 4: Permuted immanants are linear combinations of \mathcal{D} -functions (and vice versa).

Proof: Let P_σ be the permutation matrix corresponding to the permutation σ . Depending on whether P_σ acts on the left or the right of a matrix M , either the rows or columns of M get permuted. In this proof, P_σ acts on the left, which permutes the rows. To prove this lemma, Theorem 2 is applied to a row-permuted matrix $P_\sigma M$:

$$\text{imm}^\lambda(P_\sigma M) = \sum_i \mathcal{D}_{i,i}^\lambda(P_\sigma M) \quad (55)$$

$$= \sum_i \langle \psi_i^\lambda | D_\lambda(P_\sigma) D_\lambda(M) | \psi_i^\lambda \rangle = \sum_{ij} \mathcal{D}_{i,j}^\lambda(P_\sigma) \mathcal{D}_{j,i}^\lambda(M). \quad (56)$$

Note that the coefficients $\mathcal{D}_{ij}^\lambda(P_\sigma) = \langle \psi_i^\lambda | D_\lambda(P_\sigma) | \psi_j^\lambda \rangle$ are the standard (Yamanouchi) entries [53] for the matrix representation of P_σ in the representation λ of \mathfrak{S}_n . From the above computation, we see that an immanant of $P_\sigma M$ is a linear combination of \mathcal{D} -functions, which in turn means that all the entries of $\mathcal{D}^\lambda(M)$ are linear combinations of permuted λ -immanants. In particular,

\mathcal{D} -function Notation	Polynomial in Z entries
$\mathcal{D}_{1,1}^{\mathbb{H}}(Z)$	$Z_{11}Z_{22}Z_{33} - Z_{12}Z_{21}Z_{33} - Z_{13}Z_{22}Z_{31}$ $- Z_{11}Z_{23}Z_{32} + Z_{12}Z_{23}Z_{31} + Z_{13}Z_{21}Z_{32}$
$\mathcal{D}_{1,1}^{\mathbb{H}\mathbb{H}}(Z)$	$Z_{11}Z_{22}Z_{33} + Z_{12}Z_{21}Z_{33} + Z_{13}Z_{22}Z_{31}$ $+ Z_{11}Z_{23}Z_{32} + Z_{12}Z_{23}Z_{31} + Z_{13}Z_{21}Z_{32}$
$\mathcal{D}_{1,1}^{\mathbb{H}\mathbb{H}\mathbb{H}}(Z)$	$\frac{1}{2}(-Z_{13}Z_{22}Z_{31} - Z_{12}Z_{23}Z_{31} - Z_{13}Z_{21}Z_{32})$ $- Z_{11}Z_{23}Z_{32} + 2Z_{12}Z_{21}Z_{33} + 2Z_{11}Z_{22}Z_{33})$
$\mathcal{D}_{1,2}^{\mathbb{H}\mathbb{H}}(Z)$	$\frac{\sqrt{3}}{2}(-Z_{13}Z_{22}Z_{31} - Z_{12}Z_{23}Z_{31}$ $+ Z_{13}Z_{21}Z_{32} + Z_{11}Z_{23}Z_{32})$
$\mathcal{D}_{2,1}^{\mathbb{H}\mathbb{H}}(Z)$	$\frac{\sqrt{3}}{2}(-Z_{13}Z_{22}Z_{31} + Z_{12}Z_{23}Z_{31}$ $- Z_{13}Z_{21}Z_{32} + Z_{11}Z_{23}Z_{32})$
$\mathcal{D}_{2,2}^{\mathbb{H}\mathbb{H}}(Z)$	$\frac{1}{2}(Z_{13}Z_{22}Z_{31} - Z_{12}Z_{23}Z_{31} - Z_{13}Z_{21}Z_{32}$ $Z_{11}Z_{23}Z_{32} - 2Z_{12}Z_{21}Z_{33} + 2Z_{11}Z_{22}Z_{33})$

TABLE II. Group functions $\mathcal{D}_{ij}^\lambda(Z)$ of Eq. (51) connecting $(1, 1, 1)$ - states in $GL_3(\mathbb{C})$.

for an arbitrary matrix, this corollary shows that of the total $n!$ possible permuted immanants, there are exactly s_λ^2 linearly independent permuted immanants of shape λ , as there are that many \mathcal{D} -functions. \square

We give an example for the 3-fermion case, where the above lemma implies that every element of $\mathfrak{R}^\lambda(\bar{\tau})$ is a linear combination of permuted immanants of the delay matrix $r(\bar{\tau})$. To simplify notation, λ_σ^M is used to denote the λ -immanant of the matrix M whose rows are permuted by σ , that is, row i is replaced by row $\sigma(i)$. There are $3! = 6$ permuted immanants, but as we have shown, only a linear combination of s_λ^2 of them are needed to write an entry of $\mathfrak{R}^\lambda(\bar{\tau})$; we choose the permutations e , (12), (23), and (132). The entries of $\mathfrak{R}(\bar{\tau}; f)$ that appear in Eq. (48) as both a linear combination of permuted immanants and as a \mathcal{D} -function are given in Table III.

In Table III, the equality $r_{ij}(\bar{\tau}) = r_{ji}(\bar{\tau})$ has been used to simplify the polynomials. Notice how $\mathfrak{R}_{1,2}^{\mathbb{H}\mathbb{H}}(\bar{\tau}) = \mathfrak{R}_{2,1}^{\mathbb{H}\mathbb{H}}(\bar{\tau})$ and that there are 5 distinct functions that appear in the in the block-diagonalized rate matrix. In the general case the rate matrix is a real symmetric matrix, so its block-diagonal form is also be symmetric. To determine the number of distinct functions we simply need to count the number of entries on or above the main diagonal in $\mathfrak{R}^\lambda(\bar{\tau})$ for each $\lambda \vdash n$. Each $\mathfrak{R}^\lambda(\bar{\tau})$ matrix is of size s_λ , so by summing over all $\lambda \vdash n$ we find that the number of distinct functions in the block-diagonalized rate matrix is

$$\sum_{\lambda \vdash n} \frac{s_\lambda^2 + s_\lambda}{2} \sim \frac{n!}{2}, \quad (57)$$

as $\sum_{\lambda \vdash n} s_\lambda^2 = n!$.

The same linear transformation T that block-diagonalizes the rate matrix also acts on the scattering matrix $A(s)$. Similarly, we see that $\mathcal{D}^\lambda(A(s))$ is the matrix whose i^{th} column is $\mathbf{v}_{\lambda,i}(s)$. For the column vector $\mathbf{v}(s)$, one also easily expresses the entries in

Entry in $\mathfrak{R}(\bar{\tau}; p)$	\mathcal{D} -function Notation	Sum of Permuted Immanants	Polynomial in $r(\bar{\tau})$ entries
$\mathfrak{R}_{1,1}^{\boxplus}(\bar{\tau})$	$\mathcal{D}_{1,1}^{\boxplus}(r)$	$\det(r)$	$1 - r_{12}^2 - r_{13}^2 - r_{23}^2 + 2r_{12}r_{23}r_{31}$
$\mathfrak{R}_{1,1}^{\boxminus}(\bar{\tau})$	$\mathcal{D}_{1,1}^{\boxminus}(r)$	$\text{per}(r)$	$1 + r_{12}^2 + r_{13}^2 + r_{23}^2 + 2r_{12}r_{23}r_{31}$
$\mathfrak{R}_{1,1}^{\boxplus}(\bar{\tau})$	$\mathcal{D}_{1,1}^{\boxplus}(r)$	$\frac{1}{2} \left(\boxplus_e^r + \boxplus_{(12)}^r \right)$	$1 + r_{12}^2 - \frac{1}{2}r_{13}^2 - \frac{1}{2}r_{23}^2 - r_{12}r_{23}r_{31}$
$\mathfrak{R}_{1,2}^{\boxplus}(\bar{\tau})$	$\mathcal{D}_{1,2}^{\boxplus}(r)$	$\sqrt{3} \left(-\frac{1}{6}\boxplus_e^r + \frac{1}{3}\boxplus_{(23)}^r + \frac{1}{6}\boxplus_{(12)}^r - \frac{1}{3}\boxplus_{(132)}^r \right)$	$\frac{\sqrt{3}}{2} (r_{23}^2 - r_{13}^2)$
$\mathfrak{R}_{2,1}^{\boxplus}(\bar{\tau})$	$\mathcal{D}_{2,1}^{\boxplus}(r)$	$\sqrt{3} \left(-\frac{1}{6}\boxplus_e^r + \frac{1}{3}\boxplus_{(23)}^r + \frac{1}{6}\boxplus_{(12)}^r - \frac{1}{3}\boxplus_{(132)}^r \right)$	$\frac{\sqrt{3}}{2} (r_{23}^2 - r_{13}^2)$
$\mathfrak{R}_{2,2}^{\boxplus}(\bar{\tau})$	$\mathcal{D}_{2,2}^{\boxplus}(r)$	$\frac{1}{2} \left(\boxplus_e^r - \boxplus_{(12)}^r \right)$	$1 - r_{12}^2 + \frac{1}{2}r_{13}^2 + \frac{1}{2}r_{23}^2 - r_{12}r_{23}r_{31}$

TABLE III. Explicit expressions of various $\mathfrak{R}_{ij}^{\lambda}(\bar{\tau})$ for $n = 3$ particles. The argument $\bar{\tau}$ is implicit in r or r_{ij} .

terms of permuted immanants or \mathcal{D} -functions:

$$\begin{bmatrix} \mathbf{v}_{\boxminus;1}(s) \\ \mathbf{v}_{\boxplus;1}(s) \\ \mathbf{v}_{\boxplus;1}^1(s) \\ \mathbf{v}_{\boxplus;1}^2(s) \\ \mathbf{v}_{\boxplus;2}^1(s) \\ \mathbf{v}_{\boxplus;2}^2(s) \end{bmatrix} = \begin{bmatrix} \frac{1}{\sqrt{6}}\boxminus\boxminus\boxminus A(s) \\ \frac{1}{\sqrt{6}}\boxplus\boxplus\boxplus A(s) \\ \frac{1}{2\sqrt{3}} \left(\boxplus_e^{A(s)} + \boxplus_{(12)}^{A(s)} \right) \\ -\frac{1}{6}\boxplus_e^{A(s)} + \frac{1}{3}\boxplus_{(23)}^{A(s)} + \frac{1}{6}\boxplus_{(12)}^{A(s)} - \frac{1}{3}\boxplus_{(132)}^{A(s)} \\ \frac{1}{6}\boxplus_e^{A(s)} + \frac{1}{3}\boxplus_{(23)}^{A(s)} + \frac{1}{6}\boxplus_{(12)}^{A(s)} + \frac{1}{3}\boxplus_{(132)}^{A(s)} \\ \frac{1}{2\sqrt{3}} \left(\boxplus_e^{A(s)} - \boxplus_{(12)}^{A(s)} \right) \end{bmatrix} = \begin{bmatrix} \frac{1}{\sqrt{6}}\mathcal{D}_{\boxminus\boxminus\boxminus}(A(s)) \\ \frac{1}{\sqrt{6}}\mathcal{D}_{\boxplus\boxplus\boxplus}(A(s)) \\ \frac{1}{\sqrt{3}}\mathcal{D}_{\boxplus;1}^{\boxplus}(A(s)) \\ \frac{1}{\sqrt{3}}\mathcal{D}_{\boxplus;1}^{\boxplus}(A(s)) \\ \frac{1}{\sqrt{3}}\mathcal{D}_{\boxplus;2}^{\boxplus}(A(s)) \\ \frac{1}{\sqrt{3}}\mathcal{D}_{\boxplus;2}^{\boxplus}(A(s)) \end{bmatrix} \quad (58)$$

In general, the entries of $\mathbf{v}_{\lambda;i}(s)$ are group functions multiplied by the scaling factor $\sqrt{s_{\lambda}/n!}$, where $s_{\lambda} = \dim(\lambda)$ is the dimension of the irrep λ of \mathfrak{S}_n .

Lemma 5: Assume s with $s_i = 0$ or 1, and let $r(\bar{\tau})$ be the $n \times n$ delay matrix and $\mathfrak{R}^{\lambda}(\bar{\tau})$ be a block that carries the λ -representation of \mathfrak{S}_n in the block diagonalization of the rate matrix. If $\text{imm}^{\lambda}(r(\bar{\tau})) = 0$, then every entry of the matrix $\mathfrak{R}^{\lambda}(\bar{\tau})$ is also 0.

Proof: Begin by assuming that $\text{imm}^{\lambda}(r(\bar{\tau})) = 0$. Applying Theorem 2 to the delay matrix, it follows that the trace of $\mathfrak{R}^{\lambda}(\bar{\tau})$ is 0. From Eqs. (29) and (30), the rate matrix $R(\bar{\tau}; p)$ is clearly a Gram matrix, and remains as such under the change of basis generated by the similarity transformation T that brings it to block diagonal form. Thus $\mathfrak{R}^{\lambda}(\bar{\tau})$ is a Gram matrix and has non-negative eigenvalues. Since the trace of a matrix is the sum of its eigenvalues, the trace of $\mathfrak{R}^{\lambda}(\bar{\tau})$ is 0, and $\mathfrak{R}^{\lambda}(\bar{\tau})$ has all non-negative eigenvalues, it follows that all the eigenvalues of $\mathfrak{R}^{\lambda}(\bar{\tau})$ are zero. Since all the eigenvalues of $\mathfrak{R}^{\lambda}(\bar{\tau})$ are zero, it must be nilpotent; however, $\mathfrak{R}^{\lambda}(\bar{\tau})$ is also symmetric and it's well-known that the only matrix that is both symmetric and nilpotent is the zero matrix. \square

Lemma 5 thus establishes a simple test to determine which $\mathfrak{R}^{\lambda}(\bar{\tau})$ are 0, thus truncating the sum in Eqs. (49) or (50).

D. Fully distinguishable particles

There remains an important case to examine: the situation where some particles are fully distinguishable. This occurs when $r_{ij}(\bar{\tau}) = r_{ji}(\bar{\tau}) = 0$ in the matrix $r(\bar{\tau})$. In this section we first show how this limit can modify our block diagonalization algorithm to provide significant simplifications, and discuss next if this limit is realizable within our time-overlap model to compute r_{ij} for $i \neq j$.

We first investigate the modification to our scheme by supposing one particle is fully distinguishable from all the rest. For definiteness, take this to be the particle number k . Then the entries $r_{ik}(\bar{\tau})$ and $r_{ki}(\bar{\tau})$ of the matrix $r(\bar{\tau})$ will be 0 except for $r_{kk}(\bar{\tau}) = 1$; the matrix $r(\bar{\tau})$ is thus block diagonal. The matrix $R(\bar{\tau})$ will also be block diagonal so that after suitable permutations of rows and columns, it can be brought to a form with n identical blocks explicitly repeated. Our previous procedure then amounts to further block diagonalization inside each of the repeated blocks using representations of \mathfrak{S}_{n-1} rather than \mathfrak{S}_n .

If two particles are fully distinguishable - say particle number k and particle number q - one simply applies the same observation as previously to particle number q , thereby reducing the problem to multiple copies of the \mathfrak{S}_{n-2} problem. Obviously, as the number of fully distinguishable particles increases, the size of each non-trivial block in the matrix R decreases, until eventually one reaches the case where all particles are fully distinguishable: this is a ‘‘classical’’ limit. In this case, the entries $r_{ij}(\bar{\tau})$ of the matrix $r(\bar{\tau})$ are δ_{ij} , and the rate matrix $R(\bar{\tau})$ is already diagonal: there is thus no need to block diagonalize $R(\bar{\tau})$.

For instance, if we have $n = 3$ fermions and the last particle is fully distinguishable, then

$$r(\bar{\tau}) = \begin{pmatrix} 1 & r_{12}(\bar{\tau}) & 0 \\ r_{21}(\bar{\tau}) & 1 & 0 \\ 0 & 0 & 1 \end{pmatrix}, \quad (59)$$

and, after suitable rearrangement of rows and columns, we reach

$$R(\bar{\tau}; \mathbf{f}) = \begin{pmatrix} 1 & -r_{12}^2(\bar{\tau}) & 0 & 0 & 0 & 0 \\ -r_{12}^2(\bar{\tau}) & 1 & 0 & 0 & 0 & 0 \\ 0 & 0 & 1 & -r_{12}^2(\bar{\tau}) & 0 & 0 \\ 0 & 0 & -r_{12}^2(\bar{\tau}) & 1 & 0 & 0 \\ 0 & 0 & 0 & 0 & 1 & -r_{12}^2(\bar{\tau}) \\ 0 & 0 & 0 & 0 & -r_{12}^2(\bar{\tau}) & 1 \end{pmatrix}, \quad (60)$$

where $r_{21}(\bar{\tau}) = r_{12}^*(\bar{\tau})$ has been used. Eq. (60) is clearly 3 copies of the problem with 2 partially distinguishable fermions.

If now all particles are fully distinguishable, $r_{ij}(\bar{\tau}) = \delta_{ij}$ so that $r(\bar{\tau})$ and $R(\bar{\tau}; \mathbf{p})$ are both unit matrices: there is no need for block diagonalization. In this case the rate collapses to

$$\sum_i |v_i(s)|^2 = \sum_{\gamma \in \mathfrak{S}_3} |\mathbf{A}_{(\gamma)}(s)|^2 = \sum_{\gamma \in \mathfrak{S}_3} |A_{1\gamma(1)}(s)|^2 |A_{2\gamma(2)}(s)|^2 |A_{3\gamma(3)}(s)|^2 \quad (61)$$

which can be seen to be the permanent of the non-negative $n \times n$ matrix with entries $|A_{ij}(s)|^2$. In this case, one can use an efficient algorithm [54] to evaluate the permanent of this type of matrix as long as a small amount of error is allowed.

We now ask if it is possible to obtain $r_{ij} = \delta_{ij}$ for all particles in our model when computing r_{ij} as the temporal overlap $e^{-\delta\omega^2(\tau_i - \tau_j)^2/2}$. For simplicity, we imagine each pulse separated from the one ahead of it by some fixed interval $\Delta T = \tau_{i+1} - \tau_i$, independent of i . Thus, under this assumption, we have $(\tau_i - \tau_j)^2 = (i - j)^2 \Delta T^2$. We note that, for n particles, the total integration time is $\mathcal{T} \sim n\Delta T$, so using $\mathcal{T}\Delta\Omega \approx 2\pi$ for Fourier-limited detectors yields

$$(\tau_i - \tau_j)^2 = \frac{(i - j)^2 \mathcal{T}^2}{n^2} \sim \frac{4\pi^2(i - j)^2}{n^2(\Delta\Omega)^2}, \quad (62)$$

$$\delta\omega^2(\tau_i - \tau_j)^2 \sim \frac{\Delta\omega^2}{\Delta\omega^2 + \Delta\Omega^2} \frac{4\pi^2(i - j)^2}{n^2}. \quad (63)$$

It will be convenient to use $1/\Delta\omega$, the inverse frequency width of the pulse, as the timescale for our problem. For long integration times $\mathcal{T} \sim 2\pi/\Delta\Omega \gg 1/\Delta\omega$, or $\Delta\omega \gg \Delta\Omega/2\pi$, and Eq.(63) becomes

$$\delta\omega^2(\tau_i - \tau_j)^2 \approx \frac{4\pi^2(i - j)^2}{n^2}, \quad (\text{for } \mathcal{T} \gg 1/\Delta\omega), \quad (64)$$

which is appreciable only if $|i - j|/n \approx 1$, *i.e.* for ‘‘very distant’’ pulses in a sequence of $n \gg 1$ pulses. However, for ‘‘nearly neighbouring pulses’’ and sufficiently large number of fermions, so that $|i - j| \ll n$, we have $\frac{4\pi^2(i - j)^2}{n^2} \ll 1$ and hence

$$e^{-\delta\omega^2(\tau_i - \tau_j)^2} \approx 1 - \frac{4\pi^2(i - j)^2}{n^2}, \quad (\text{for } |i - j| \ll n). \quad (65)$$

Thus we conclude that we cannot reach the limit where all $r_{ij} = \delta_{ij}$ for long integration times even if the pulses are well separated in time.

Next consider short integration times, for which $\mathcal{T} \ll 1/\Delta\omega$, or $\Delta\Omega \gg 2\pi\Delta\omega$. In this case

$$\delta\omega^2(\tau_i - \tau_j)^2 \sim \frac{(2\pi\Delta\omega)^2}{\Delta\Omega^2} \frac{(i-j)^2}{n^2} \ll 1, \quad (\text{for } \mathcal{T} \ll 1/\Delta\omega, \text{ any } |i-j|), \quad (66)$$

always. Here again, it is not possible reach the limit where $r_{ij} = \delta_{ij}$.

Hence, we conclude that, for Fourier-limited detectors, we cannot reach a regime where all particles are considered fully distinguishable. Instead we reach this regime by sending particles one by one at times $t_n = n\Delta T$ but detecting after a time $\approx (n + \frac{1}{2})\Delta T$; in this case the particles are detected one by one, and never detected in coincidence.

One could instead imagine an alternate model where the r_{ij} 's are not measured by a temporal overlap, but by a polarization overlap, *i.e.* working with polarized fermions. One then easily shows that $r_{ij} = \cos^2(\theta_{ij})$, where θ_{ij} is the relative angle of the polarization vectors for particles i and j . In such a scenario, it is clearly not possible to have more than two particles which are pairwise fully distinguishable, and it is not possible to reach the limit where all $r_{ij} = \delta_{ij}$ either.

V. DISCRETIZING TIME AND GAMAS'S THEOREM

Although arrival times are continuous in principle, and hence range over any real value in some interval, in practice arrival times are discrete due to resolution limits of delay lines. In this section, we exploit discretization to write arrival times as a tuple of integers, with each integer in the tuple denoting the arrival time of the corresponding particle at the detector. Absolute arrival times are not needed and we use relative arrival times to introduce the delay partition. Next we explain how these partitions can be partially ordered, which sets the stage for introducing and using Gamas's theorem. Finally, we use these rules for partitioning to restrict sums used for computing the coincidence rate equations. Here again the discussion applies any s with $s_i = 0$ or 1 , and we assume that no one particle is fully distinguishable from any of the others.

A. Discretizing time and the delay partition

In the remainder of the paper, we use the combinatorics of Young diagrams to show that when some of the $|\bar{\tau}_i - \bar{\tau}_j| \approx 0$, some of the terms in Eqs. (49) and (50) are in turn automatically 0, thus further simplifying the actual calculation by truncating the sum.

If the arrival times are controlled to arbitrary precision, the exact rate is given by Eq. (34). In practice, we envisage a scenario where, if $|\bar{\tau}_i - \bar{\tau}_j| < \varepsilon$, the incident particles are considered to arrive simultaneously and thus indistinguishable. It is then convenient to imagine that the source supplies, for each run, n particles arriving within some finite time interval \mathcal{T} . This total time interval is divided into a number $b \geq 2$ of discrete identical time bins of with $\varepsilon = \mathcal{T}/b$, so that a particle arriving at time $\bar{\tau}_i$ is assigned the discrete arrival time τ_c

$$\bar{\tau}_i \rightarrow \tau_c \quad \text{when} \quad \frac{(c-1)\mathcal{T}}{b} \leq \bar{\tau}_i < \frac{c\mathcal{T}}{b}, \quad c = 1, \dots, b. \quad (67)$$

The next step is construct a *delay partition* μ_τ given a vector τ containing discretized arrival times. This is done by simply tallying the number of particles in each bin, removing bins with no particles, and ordering the counts in decreasing order. Thus, if there are $b = 12$ bins, there are 12 possible discrete values of τ_i for each particle. If additionally there are $n = 4$ particles, the discrete arrival-time vector is $\tau = [\tau_1, \tau_4, \tau_1, \tau_9]$, we assign to this arrival-time vector τ the delay partition $\mu_\tau = (2, 1, 1)$.

The delay partition is determined only by the tally in each bin, irrespective of the index of the (discretized) arrival times τ_i and irrespective of the actual bin in which τ_i falls. The (discrete) arrival-time vectors

$$[\tau_2, \tau_1, \tau_1, \tau_6], \quad [\tau_7, \tau_3, \tau_4, \tau_3], \quad [\tau_5, \tau_5, \tau_2, \tau_{11}] \quad (68)$$

for instance all map to the same delay partition $\mu_\tau = (2, 1, 1)$. In this way a delay partition is an equivalence class of discrete arrival-time vectors, and all the previous partitions are equivalent to the arrival-time vector $[\tau_1, \tau_1, \tau_2, \tau_3]$. For $n = 4$ and $b \geq 4$, we have the following possible delay partitions:

$$\begin{aligned} [\tau_1, \tau_1, \tau_1, \tau_1] &\rightarrow \mu_\tau = \square\square\square\square \\ [\tau_1, \tau_1, \tau_1, \tau_2] &\rightarrow \mu_\tau = \square\square\square \\ [\tau_1, \tau_1, \tau_2, \tau_2] &\rightarrow \mu_\tau = \square\square \\ [\tau_1, \tau_1, \tau_2, \tau_3] &\rightarrow \mu_\tau = \square\square \\ [\tau_1, \tau_2, \tau_3, \tau_4] &\rightarrow \mu_\tau = \square \end{aligned} \quad (69)$$

B. Dominance Ordering and Gamas's theorem

For a given delay partition, one can obtain a significant simplification in the evaluation of the coincidence rate equations. This simplification is a consequence of Gamas's theorem, from which one deduces that some immanants of a Gram matrix are zero based on dominance ordering of partitions.

Dominance ordering is a partial ordering of partitions, given by $\mu \trianglelefteq \lambda$ when

$$\mu_1 + \mu_2 + \dots + \mu_i \leq \lambda_1 + \lambda_2 + \dots + \lambda_i \tag{70}$$

for all $i \geq 1$. We say that two partitions cannot be compared when neither one dominates the other. The notation $\mu \triangleleft \lambda$ means that λ strictly dominates μ (a partition dominates itself, but it doesn't strictly dominate itself). An example is given in Fig. 2, where it can be seen that $\square\square\square\square$ dominates all partitions of 6 and that $\square\square\square$ and $\square\square\square$ cannot be compared.

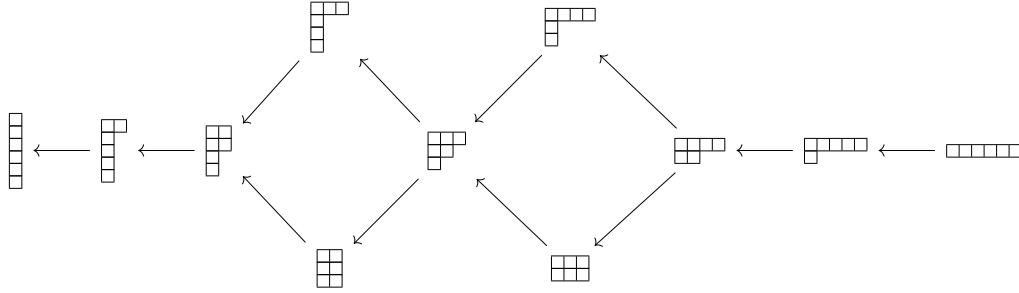


FIG. 2. The dominance ordering of the partitions of 6.

Gamas's theorem tells us whether the λ -immanant of a Gram matrix is zero by looking at the shape of the partition λ . The theorem is stated as follows.

Theorem 6: (Gamas [33]): Let $V_{ij} = \langle f_i | f_j \rangle$ be a $n \times n$ Gram matrix formed by the set of basis vectors $\{f_i\}$, and let $\lambda \vdash n$ be a partition. We have that $\text{imm}^\lambda(V) \neq 0$ if and only if the columns of λ can partition the set of basis vectors $\{f_i\}$ into linearly independent sets.

In Table IV, a 0 indicates that the immanant, for the corresponding set of basis functions, is 0. Gamas's theorem is a bi-conditional statement, so the blank boxes mean the corresponding immanant is non-zero. For further reading on Gamas's theorem see [34].

											$f_1 f_2 f_3 f_4 f_5 f_6$
0											$f_1 f_1 f_2 f_3 f_4 f_5$
0	0										$f_1 f_1 f_2 f_2 f_3 f_4$
0	0	0		0							$f_1 f_1 f_2 f_2 f_3 f_3$
0	0	0	0								$f_1 f_1 f_1 f_2 f_3 f_4$
0	0	0	0	0							$f_1 f_1 f_1 f_2 f_2 f_3$
0	0	0	0	0	0		0				$f_1 f_1 f_1 f_2 f_2 f_2$
0	0	0	0	0	0	0					$f_1 f_1 f_1 f_1 f_2 f_3$
0	0	0	0	0	0	0	0				$f_1 f_1 f_1 f_1 f_2 f_2$
0	0	0	0	0	0	0	0	0			$f_1 f_1 f_1 f_1 f_1 f_2$
0	0	0	0	0	0	0	0	0	0		$f_1 f_1 f_1 f_1 f_1 f_1$

TABLE IV. The vanishing behaviour of the immanants of 6×6 Gram matrices.

C. Restricting the sum in the coincidence rate equations.

Applying a corollary of Gamas's theorem [55] to Lemma 5 yields the following:

Proposition 7: Assume s with $s_i = 0$ or 1 . The matrix $\mathfrak{R}^\lambda(\tau)$ is non-zero if and only if λ dominates μ_τ in the dominance ordering of partitions. Thus, for a given set of discrete arrival times τ , the coincidence rate equations simplify to

$$\text{rate}(\tau, s; \mathbf{b}) = \sum_{\mu_\tau \leq \lambda} \sum_{i=1}^{s_\lambda} v_{\lambda; i}^\dagger(s) \mathfrak{R}^\lambda(\tau) v_{\lambda; i}(s), \quad (71)$$

$$\text{rate}(\tau, s; \mathbf{f}) = \sum_{\mu_\tau \leq \lambda} \sum_{i=1}^{s_\lambda} v_{\lambda; i}^\dagger(s) \mathfrak{R}^{\lambda^*}(\tau) v_{\lambda; i}(s). \quad (72)$$

The sum is over all partitions $\lambda \vdash n$ that dominate μ_τ .

We note that if every particle arrives in a different time bin, there is no truncation and we recover the full sums of Eqs.(49) and (50).

Example 8: Consider the set of discrete arrival times $\tau = [\tau_1, \tau_1, \tau_1, \tau_2, \tau_2, \tau_2]$, corresponding to the delay partition $\mu_\tau = \square\square$. It follows that for λ equal to $\square\square\square$, $\square\square\square$, $\square\square\square$, $\square\square\square$, $\square\square\square$, $\square\square\square$, and $\square\square\square$ the $\mathfrak{R}^\lambda(\tau)$ terms are equal to zero since these are the partitions which do not dominate $\square\square$. The coincidence rate equations are thus

$$\begin{aligned} \text{rate}(\tau, s; \mathbf{b}) &= v_{\square\square\square; 1}^\dagger(s) \mathfrak{R}^{\square\square\square}(\tau) v_{\square\square\square; 1}(s) + \sum_{i=1}^5 v_{\square\square\square; i}^\dagger(s) \mathfrak{R}^{\square\square\square}(\tau) v_{\square\square\square; i}(s) \\ &\quad + \sum_{i=1}^9 v_{\square\square\square; i}^\dagger(s) \mathfrak{R}^{\square\square\square}(\tau) v_{\square\square\square; i}(s) + \sum_{i=1}^5 v_{\square\square\square; i}^\dagger(s) \mathfrak{R}^{\square\square\square}(\tau) v_{\square\square\square; i}(s), \end{aligned} \quad (73)$$

$$\begin{aligned} \text{rate}(\tau, s; \mathbf{f}) &= v_{\square\square\square; 1}^\dagger(s) \mathfrak{R}^{\square\square\square}(\tau) v_{\square\square\square; 1}(s) + \sum_{i=1}^5 v_{\square\square\square; i}^\dagger(s) \mathfrak{R}^{\square\square\square}(\tau) v_{\square\square\square; i}(s) \\ &\quad + \sum_{i=1}^9 v_{\square\square\square; i}^\dagger(s) \mathfrak{R}^{\square\square\square}(\tau) v_{\square\square\square; i}(s) + \sum_{i=1}^5 v_{\square\square\square; i}^\dagger(s) \mathfrak{R}^{\square\square\square}(\tau) v_{\square\square\square; i}(s). \end{aligned} \quad (74)$$

VI. FERMIONIC RATES AND PARTIAL DISTINGUISHABILITY

For fully indistinguishable fermions, the coincidence rate is given by the first term in Eq. (50) and contains only the modulus squared of the determinant of the matrix $A(s)$; for this case the matrix $r(\bar{\tau})$ is the unit matrix and the permanent of $R(\tau) = n!$. Since determinants can be evaluated efficiently, the evaluation of fermionic rates in this case is simple.

As we increase the distinguishability of the fermions, the expression for the coincidence rate lengthens to contain an increasing number of group functions, as per Proposition 7. Moreover, which group functions occur is determined by Gammas's theorem and the delay partition obtained from the times of arrival.

In this section we show that, once we reach a situation where at most $\lfloor \frac{n}{2} \rfloor$ fermions are pairwise indistinguishable, the expression for the coincidence rate will contain specific group functions that are evaluated, using the algorithm of [56], in a number of operations that grows exponentially with the number of fermions. We further show that, if the times of arrival are uniformly random, one must evaluate these expensive groups functions with probability differing from 1 by a number decreasing exponentially with the number of fermions. In this section we suppose again that s is such that $s_i = 0$ or 1 .

A. The Witness Partition

We begin this section by defining the witness partition and proving a lemma.

Definition 9: The witness partition μ_w is

$$\mu_w := \begin{cases} \left(\frac{n}{2}, \frac{n}{2} \right) & \text{for } n \text{ even,} \\ \left(\frac{n+1}{2}, \frac{n-1}{2} \right) & \text{for } n \text{ odd.} \end{cases} \quad (75)$$

We will often refer to the conjugate of the witness partition, which is

$$\mu_w^* = \begin{cases} (2, 2, \dots, 2) & \text{for } n \text{ even,} \\ (2, 2, \dots, 2, 1) & \text{for } n \text{ odd.} \end{cases} \quad (76)$$

Consider the case of fermionic interferometry. We present the following lemma.

Lemma 10: When n is even, group functions of type μ_w^* of the matrix $A(s)$ need to be computed to evaluate the fermionic coincidence rate equation if and only if at most $\frac{n}{2}$ of the times of arrival are contained in a single time bin, and we assume that no one particle is fully distinguishable from any of the others.

When n is odd, group functions of type μ_w^* of the matrix $A(s)$ need to be computed to evaluate the fermionic coincidence rate equation if and only if at most $\frac{n+1}{2}$ of the times of arrival are contained in a single time bin, and we assume that no one particle is fully distinguishable from any of the others.

Proof: From Eq. (72), we observe that if $\mu_\tau \leq \lambda$, then group functions of type λ^* of the matrix $A(s)$ appear in the fermionic coincidence rate equation; otherwise, we have that when λ *doesn't* dominate μ_τ (meaning that either $\lambda \triangleleft \mu_\tau$ or the two partitions cannot be compared), then group functions of type λ^* of the matrix $A(s)$ *do not* appear in the fermionic coincidence rate equation.

First, consider the case where n is even and assume that group functions of type μ_w^* appear in the fermionic rate equation. It follows that μ_w dominates the delay partition: $\mu_\tau \leq \mu_w$. The partition μ_w is of the form $(\frac{n}{2}, \frac{n}{2})$, thus μ_w dominates all partitions of width at most $\frac{n}{2}$. By construction, the partitions of width at most $\frac{n}{2}$ correspond to the instances where at most $\frac{n}{2}$ fermions are in a single time bin. Each implication in our argument is bi-conditional, so the result for even n follows.

In the case where n is odd, μ_w is now of the form $(\frac{n+1}{2}, \frac{n-1}{2})$. It's clear that μ_w dominates all of the partitions of width at most $\frac{n+1}{2}$. The rest of the proof is identical to the even case. \square

Note that regardless of whether the number of fermions is odd or even, if at most $\lceil \frac{n}{2} \rceil$ of the times of arrival are in the same time bin, then group functions of type μ_w^* of the matrix $A(s)$ need to be evaluated to determine the fermionic rate.

We proceed by showing that *some* group functions of type μ_w^* are computationally expensive to evaluate. Bürgisser [56] shows that the number of arithmetic operations needed to evaluate the immanant of Eq. (8) in the $\lambda \vdash n$ representation of $GL_n(\mathbb{C})$ is $\mathcal{O}([\text{mult}(\lambda) + \log(n)]n^2 s_\lambda d_\lambda)$. The sum in Eq. (8) contains exactly s_λ terms, so at least one of the $\mathcal{D}_{i,i}^\lambda(A(s))$ must evaluate in at least

$$\mathcal{O}([\text{mult}(\lambda) + \log(n)]n^2 d_\lambda). \quad (77)$$

operations. Here, s_λ is both the number of standard Young tableaux of shape λ and the dimension of the weight $(1, 1, 1, \dots, 1)$ subspace of the λ -irrep of $GL_n(\mathbb{C})$ and d_λ is both the number of semi-standard Young tableaux of shape λ and the dimension of the λ -irrep of $GL_n(\mathbb{C})$, $\text{mult}(\lambda)$ is the multiplicity of the highest weight λ [56]. Furthermore, *any* arithmetic algorithm that evaluates group functions of type λ “requires at least d_λ nonscalar operations” according to Theorem 5.1 of [56].

We now compute $d_{\mu_w^*}$ to get a lower bound for Eq. (77). Suppose n is even so that $\mu_w^* = (2, 2, \dots, 2)$. Exponents are used to denote repeated entries, so the partition can be more compactly written as $\mu_w^* = (2^{n/2})$. Then one easily shows that $s_{(2^{n/2})}$ is given by the Catalan number

$$C_{n/2} = \frac{1}{\frac{n}{2} + 1} \binom{n}{\frac{n}{2}} \sim \frac{2^{n+3/2}}{\sqrt{\pi n^3}} \quad (78)$$

for large n so the number of terms to evaluate is growing exponentially with the number of fermions. Moreover, the dimension of the irrep $d_{(2^{n/2})}$ of $GL_n(\mathbb{C})$ is given by

$$d_{(2^{n/2})} = \binom{n}{\frac{n}{2}} \binom{n+1}{\frac{n}{2}} \frac{1}{\frac{n}{2} + 1} = C_{n/2} \binom{n+1}{\frac{n}{2}}. \quad (79)$$

The binomial coefficient $\binom{n+1}{\frac{n}{2}} \sim 2^{n+3/2} e^{-1/(2n+2)} / \sqrt{(n+1)\pi}$ for large n so that, altogether:

$$d_{(2^{n/2})} \approx \frac{2^{2n+3}}{n^2 \pi} \quad (80)$$

also scales exponentially with the number of fermions. Thus, at least one of the group functions necessary to compute the fermionic coincidence rate equation requires a number of arithmetic operations that scales exponentially with the number of fermions. A similar expression and argument can be made when n is odd. Thus, combining this with Theorem 5.1 of [56] as discussed above, we have thus shown the following.

Proposition 11: If at most $\lceil \frac{n}{2} \rceil$ of the times of arrival are contained in any one time bin, and no particle is fully distinguishable from any other, then our procedure for the exact computation of the fermionic coincidence rate equation requires a number of arithmetic operations that scales exponentially in the number of fermions.

B. Probability of the witness partition appearing for uniformly-random arrival times

In this subsection, we discuss a simple model where the discretized arrival times are uniformly random over some interval \mathcal{I} . Fix some string s where $s_i = 0$ or 1 . Imagine n possible uniformly random discrete arrival times (one per particle) distributed over a total of b time bins. The arrival times can be repeated. Given a delay partition $\mu_\tau = (\mu_1, \mu_2, \dots, \mu_k)$, we need to find how many ways we can distribute the n particles in b bins so that μ_1 are in any one bin, μ_2 are in any other bin which is not the first, etc.

For instance, if $n = 6$ and $b = 8$, then the arrival times could be $\tau = [1, 5, 8, 5, 8, 3]$. For clarity we tabulate the results:

particle #	1	2	3	4	5	6
bin #	1	5	8	5	8	3

TABLE V. Tabulated results of a hypothetical experiment.

This arrival time vector τ is associated to the delay partition $\mu_\tau = (2, 2, 1, 1)$. Let b_i denote the number of time bins that contain exactly i particles. In this example, the fifth and eighth time bins contain two particles each, so $b_2 = 2$; the first and third time bins contain one particle, so $b_1 = 2$; the second, fourth, sixth, and seventh time bins contain no particles, so $b_0 = 4$. In general, the b_i terms satisfy the following constraints

$$\begin{aligned} \sum_{i=0}^n b_i &= b \\ \sum_{i=0}^n i b_i &= n. \end{aligned} \quad (81)$$

With b time bins and n particles there are b^n possible ways for the particles to arrive at the detectors; assuming that each of these possibilities are equally likely, we present an expression for the probability that a random input of particles has a particular delay partition.

Proposition 12: In an experiment with n particles and b time bins, the probability that a uniformly-random set of arrival times has delay partition $\mu_\tau = (\mu_1, \mu_2, \dots, \mu_k)$ is

$$\mathcal{P}(\mu_\tau; b) = \frac{1}{b^n} \binom{n}{\mu_1, \mu_2, \dots, \mu_k} \binom{b}{b_0, b_1, \dots, b_n}, \quad (82)$$

where the b_i 's are computed from the delay partition μ_τ as described above. If b is less than the number of parts k of a delay partition, then the probability of that delay partition occurring is 0.

Example 13: Suppose there are 8 time bins, 5 particles, and we are computing the probability of the delay partition $\mu_\tau = (2, 2, 1)$ occurring. Of the 8 time bins, there is 1 bin that contains 1 particle, 2 bins that contain 2 particles, and 5 bins that contain 0 particles; thus, $b_0 = 5, b_1 = 1, b_2 = 2$. Applying Proposition 12, we get

$$\begin{aligned} \mathcal{P}((2, 2, 1); 8) &= \frac{1}{8^5} \frac{5!}{(2!)(2!)(1!)} \frac{8!}{(5!)(1!)(2!)} \\ &= \frac{315}{2048}. \end{aligned} \quad (83)$$

Recall that Proposition 11 states that when at most $\lceil \frac{n}{2} \rceil$ of the times of arrival are contained in a single time bin, this means that our method for computing the fermionic coincidence rate equation requires exponentially many arithmetic operations. Let \mathcal{P} denote the probability of obtaining a delay partition $\mu_\tau = (\mu_1, \mu_2, \dots)$ with $\mu_1 \leq \lceil \frac{n}{2} \rceil$. We show that $1 - \mathcal{P}$, which is the probability of obtaining a delay partition with $\mu_1 > \lceil \frac{n}{2} \rceil$, approaches 0 exponentially fast with n .

We begin with the case where n is even. Let $P(B)$ be the probability of getting a delay partition with first part equal to λ_1 and the remaining parts are arbitrary, and let $P(A)$ be the probability of obtaining delay partition $\lambda' = (\lambda_2, \lambda_3, \dots, \lambda_k) \vdash n - \lambda_1$ for the remaining $n - \lambda_1$ particles being sorted into the remaining $(b - 1)$ bins. We get that the conditional probability $P(A|B)$ is given by

$$P(A|B) = \frac{1}{(b-1)^{n-\lambda_1}} \binom{n-\lambda_1}{\lambda_2, \lambda_3, \dots, \lambda_k} \binom{b-1}{b_0, b_1, \dots, b_{\lambda_1-1}, 1, b_{\lambda_1+1}, \dots, b_n}, \quad (84)$$

where $b_{\lambda_1} = 1$. The probability $P(A \cap B)$ is simply the probability of obtaining an arbitrary delay partition λ , which is given in Eq. (82). The probability $P(B)$ is thus given by the following quotient

$$\begin{aligned} \frac{P(A \cap B)}{P(A|B)} &= \frac{\frac{1}{b^n} (\lambda_1, \lambda_2, \dots, \lambda_k) (b_0, b_1, \dots, b_n)}{\frac{1}{(b-1)^{n-\lambda_1}} (\lambda_2, \lambda_3, \dots, \lambda_k) (b_0, b_1, \dots, b_{\lambda_1-1}, 1, b_{\lambda_1+1}, \dots, b_n)}, \\ &= \frac{(b-1)^{n-\lambda_1}}{b^n} \frac{n!}{\lambda_1! (n-\lambda_1)!} \frac{b!}{(b-1)!}, \\ &= \binom{n}{\lambda_1} \frac{(b-1)^{n-\lambda_1}}{b^{n-1}}. \end{aligned} \quad (85)$$

To obtain $1 - \mathcal{P}$ we need to sum over all partitions $\lambda \vdash n$ with $\lambda_1 \geq \frac{n}{2} + 1$,

$$1 - \mathcal{P} = \frac{1}{b^{n-1}} \sum_{\lambda_1 = \frac{n}{2} + 1}^n \binom{n}{\lambda_1} (b-1)^{n-\lambda_1}. \quad (86)$$

We factor out $(b-1)^n$ from each term in the sum to get

$$1 - \mathcal{P} = \frac{(b-1)^n}{b^{n-1}} \sum_{\lambda_1 = \frac{n}{2} + 1}^n \binom{n}{\lambda_1} \left(\frac{1}{b-1}\right)^{\lambda_1}. \quad (87)$$

We assume that n and b are large to be able to truncate the sum. We have

$$\begin{aligned} 1 - \mathcal{P} &= \frac{(b-1)^{n-1}}{b^{n-1}} \left(\binom{n}{n/2+1} \left(\frac{1}{b-1}\right)^{n/2} + \binom{n}{n/2+2} \left(\frac{1}{b-1}\right)^{1+n/2} + \dots \right), \\ &= \frac{(b-1)^{n-1}}{b^{n-1}} \binom{n}{n/2+1} \left(\frac{1}{b-1}\right)^{n/2} \left(1 + \frac{n-2}{n+4} \left(\frac{1}{b-1}\right) + \dots \right), \\ &\approx \frac{(b-1)^{n-1}}{b^{n-1}} \frac{2^{n+\frac{1}{2}}}{\sqrt{n\pi}} \left(\frac{1}{b-1}\right)^{n/2} \left(1 + \frac{n-2}{n+4} \left(\frac{1}{b-1}\right) + \dots \right). \end{aligned} \quad (88)$$

By assuming again that $b-1 \approx b$ and by truncating the sum after the first term, we find that

$$1 - \mathcal{P} \approx \sqrt{\frac{2}{n\pi}} \left(\frac{4}{b}\right)^{\frac{n}{2}}. \quad (89)$$

We note that when n is odd there is a near-identical expansion and we get the same estimate for the probability.

Corollary 14: In an experiment with n particles that arrive uniformly randomly in b discrete time bins, the probability \mathcal{P} of at most $\lceil \frac{n}{2} \rceil$ particles being in the same time bin is

$$\mathcal{P} \approx 1 - \sqrt{\frac{2}{n\pi}} \left(\frac{4}{b}\right)^{\frac{n}{2}}. \quad (90)$$

This is also the probability of needing to compute the (expensive) μ_w^* -group functions of $A(s)$. We observe that when $b \geq 5$, then \mathcal{P} approaches 1 exponentially fast as n increases.

VII. APPLICATIONS TO SAMPLING PROBLEMS

A. Generalized Boson and Fermion Sampling

Quantum computing focuses on technology and algorithms for solving certain computational problems more efficiently than what can be accomplished using non-quantum (i.e., ‘‘classical’’) computing, essentially based on the binary representation of

information and Boolean logic [57]. Both universal and specialized quantum computing approaches are followed. Gate-based quantum computing [58, 59] is an example of universal quantum computing. Both quantum annealing [60] and boson sampling [8, 61] are examples of specialized, purposed quantum computing that is not universal. Boson sampling is about simultaneously firing n single photons so they arrive simultaneously at detectors behind an m -channel passive optical interferometer.

BOSONSAMPLING is a hard classical problem and easy quantum problem in both exact and approximate formulations subject to assumptions. Recall from §II A that $\Phi_{m,n}$ is the set of m -tuples (s_1, \dots, s_m) so that $s_1 + \dots + s_m = n$. When the bosons are indistinguishable, the probability distribution $\mathcal{B}[\mathcal{A}]$ over $\Phi_{m,n}$ is given by [8]

$$\Pr_{\mathcal{B}[\mathcal{A}]}[s] = \frac{|\text{per}(A(s))|^2}{s_1!s_2!\dots s_m!}. \quad (91)$$

Definition 15: Given \mathcal{A} as input, the problem of BOSONSAMPLING is to sample, either exactly or approximately, from the distribution $\mathcal{B}[\mathcal{A}]$.

The exact BOSONSAMPLING problem is not efficiently solvable by a classical computer, unless the polynomial hierarchy collapses to the third level, which is an unlikely scenario based on existing results in computational complexity [8]. Despite the simplicity behind the complexity of BOSONSAMPLING in theory, experimental BOSONSAMPLING has limitations on size and on validity of assumptions needed to trust hardness results. For example, the assumptions on the perfectly indistinguishable photons are impossible to achieve in experiments: not only are photons distinguishable in their temporal and frequency profile due to imperfect single-photon source, experimental optical interferometers also introduce additional added imperfections due to unequal path length, or unwanted phase errors. Notice that such experimental imperfections, are different from the approximate BOSONSAMPLING, which permits the sampling to deviate from the perfect sampling of an ideal bosonic interferometer with indistinguishable photon sources. The computational hardness of imperfect BOSONSAMPLING is still an ongoing subject of discussion [62].

When fermions are indistinguishable, the probability distribution $\mathcal{F}[\mathcal{A}]$ over $\Phi_{m,n}$ is given, up to a constant, by [63]

$$\Pr_{\mathcal{F}[\mathcal{A}]}[s] = |\det(A(s))|^2. \quad (92)$$

As a result of the Pauli exclusion principle, two indistinguishable fermions cannot exit from the same channel so the $s_1!s_2!\dots s_m!$ factor in the denominator of Eq. (91) is replaced here by 1. From the notion of fermion interferometry, we define the associated problem of fermion sampling.

Definition 16: Given \mathcal{A} as input, the problem of FERMIONSAMPLING is to sample, either exactly or approximately, from the distribution $\mathcal{F}[\mathcal{A}]$.

The key application of FERMIONSAMPLING is solving the same types of computational problems as for BOSONSAMPLING by opening the door to integrated semiconductor circuitry as an alternative to scaling challenges inherent in photonic approaches [64, 65].

For simultaneous arrival times at the detectors, fermion coincidence rates are easy to calculate [66, 67]. As a result, fermion interferometry has not been treated as a viable contender for quantum advantage [17] since FERMIONSAMPLING can be solved in classical polynomial time [63] (unless a quantum resource is added [65]). Mathematically, the ease of FERMIONSAMPLING arises because the hard-to-solve expressions for matrix permanents arising in boson coincidence calculations are replaced by matrix determinants for fermion coincidences [4]. The trivial nature of quantum vs classical algorithms for FERMIONSAMPLING should not discourage exploiting fermion sampling for quantum computing provided that we generalize to nonsimultaneous arrival times.

In fact, in view of Proposition 11 the lack of simultaneity removes, in part or in totality, the argument that fermion sampling is uninteresting because it is efficiently simulatable. Indeed Proposition 11 suggests that, if we are to use the state-of-the-art algorithm to evaluate group functions and immanants, the evaluation of coincidence rates is exponentially expensive under reasonable conditions as to the maximum number of indistinguishable fermions. However, while the series of Eq. (72) for the *exact* rate will contain expensive group functions, we cannot guarantee that these function will have a significant contribution to the final rate.

Heyfron [68, 69] and separately Pate [70] have obtained some results on immanant inequalities which follow dominance ordering for positive semi-definite matrices, like the delay matrix $r(\tau)$ of Eq. (27), but these results don't encompass the witness partition. Stembridge [71] has also shown that immanants of totally positive matrices, like our delay matrix, are necessarily positive (see also the appendix of [72] for some immanant inequalities). Nevertheless, to understand the contribution to the rates from group functions of $A(s)$, one would also need "anticoncentration"-type results for these functions or associated immanants for these expensive functions or immanants.

Nevertheless, as a result of Proposition 11, it is natural to generalize both BOSONSAMPLING and FERMIONSAMPLING by allowing nonsimultaneous arrival times specified by the vector $\vec{\tau}$. The set $G_{m,n} \subset \Phi_{m,n}$ contains only the strings s such that $s_i = 0$

or 1 for all i . The distribution $\mathcal{B}[\mathcal{A}; \bar{\tau}]$ over $G_{m,n}$ is defined by

$$\Pr_{\mathcal{B}[\mathcal{A}; \bar{\tau}]}[s] = \text{rate}(\bar{\tau}, s; \mathbf{b}) \quad (93)$$

where $\text{rate}(\bar{\tau}, s; \mathbf{b})$ is given in Eq. (34).

Problem 17: Exact GENBOSONSAMPLING Given the $m \times n$ matrix \mathcal{A} and a length n arrival-time vector $\bar{\tau} \in \mathbb{R}^n$ as inputs, the problem of GENBOSONSAMPLING is to sample exactly from the distribution $\mathcal{B}[\mathcal{A}; \bar{\tau}]$.

In the case of fermions, the distribution $\mathcal{F}[\mathcal{A}; \bar{\tau}]$ over $G_{m,n}$ is defined by

$$\Pr_{\mathcal{F}[\mathcal{A}; \bar{\tau}]}[s] = \text{rate}(\bar{\tau}, s; \mathbf{f}) \quad (94)$$

where $\text{rate}(\bar{\tau}, s; \mathbf{f})$ is given in Eq. (36).

Problem 18: Exact GENFERMIONSAMPLING Given the $m \times n$ matrix \mathcal{A} and a length n arrival-time vector $\bar{\tau} \in \mathbb{R}^n$ as inputs, the problem of GENFERMIONSAMPLING is to sample exactly from the distribution $\mathcal{F}[\mathcal{A}; \bar{\tau}]$.

Comparing with the original definition of BOSONSAMPLING and FERMIONSAMPLING, the exact generalized definitions above admit, in addition to the inputs n for the number of fermions, the arrival-time vector $\bar{\tau} \in \mathbb{R}^n$ but with the restriction of s to strings with $s_i = 1$ or 0, and the proviso that real- and complex-number entries are admitted as floating-point numbers up to machine precision, which is important to note because we are focused on *exact* computation. This definition differs from the one proposed in [65] where simultaneity remains but the input state is no longer a single product state.

B. Calibration and Fermion Sampling

Every interferometry experiment has the problem of non-simultaneity due to “lengths . . . not [being] well-calibrated” [8]. This problem of calibration is generally regarded as ‘just’ a technical step. Geometrically, we will refer to the *landscape* for a given set of detector positions and a given interferometer as an $(n - 1)$ -dimensional surface representing the various coincidence rates in those detectors as a function of the necessary $n - 1$ relative arrival times of the n particles. Calibration is achieved by knowing the functional form, hence appearance, of this landscape, choosing some points on the domain by experimental adjustments that control arrival times, and determining the rate at the chosen points. When sufficient resolution of the times of arrival are possible, doing so over approximately $n!/2$ points (the exact number is given in Eq. (57)) in the domain, the rate for simultaneity is then inferred (in the perfect case) because enough information is available to shift and rotate the landscape so that the ‘zero’ element of the domain is known. This way of calibrating requires the fewest number of points to estimate the simultaneous-arrival coincidence rate, which is assumed in most treatments of sampling but unfortunately not completely justified in practice.

As BOSONSAMPLING is computationally hard, simulating calibration only adds a smaller computational overhead so it does not make the computational problem any easier. FERMIONSAMPLING is another beast altogether. After calibration is completed, FERMIONSAMPLING is computationally efficient so calibration is now a key theoretical issue, not ‘just’ technical. If a fermion source ejected particles at known, definite times and all fermion paths were calibrated, then non-simultaneity would be obviated, but fermion interferometers do not work that way.

We now explain how the input delay channels for the interferometer are calibrated [73]. Intuitively, consider a source that generates n particles such that only one particle is injected into each of n channels. Suppose that the source injects all n particles simultaneously, but the channel length is unknown so the particles eventually arrive at the n detectors at uniformly random times despite the promise that all particles are injected simultaneously into each channel.

Calibration is the exercise of adjusting each channel length so that they match, and successful calibration ensures that the simultaneously generated particles are guaranteed to arrive at the detectors simultaneously. If a coincidence-rate model, which depends on arrival times, is trusted, then calibration is achieved by using coincidence-rate data for different choices of input-channel delay increments and fitting coincidence rate data to the model. Then, by interpolation, the appropriate delay-increments can be inferred from the fitted model. In practice, coincidence rates for simultaneous arrival are extrema so smart search for channel delays that yield a minimum or maximum coincidence rate, as a function of channel delays, can calibrate channel delays without having to resort to model fitting.

For our exact-rate theory, discretized control of delay times between source and interferometer is accommodated here as time bins for arrival. For our analysis, time-bin width is fixed in all channels. Thus, we consider discrete arrival times rather than treating arrival time as a continuum. The number of time bins per channel is b , which is the same for each channel, and b is the ratio of the total run time for the sampling procedure to the photodetector arrival time.

We can thus think of the arrival time as a digit in base b . As n particles are in play, the arrival time is a length n string of digits in base b . For example, if b is 16, a digit could be expressed in hexadecimal, so an example of an arrival time for

particles in 8 channels could be expressed as the length 8 hexadecimal number 12B9B0A1, which is the hexadecimal representation of 314159265. Total ignorance about channel delays corresponds to the uniform prior (distribution) over all hexadecimal numbers from 0 to FFFFFFFF, which is 4294967295 in decimal.

The trusted model computes the expected coincidence rate for each choice of length-8 hexadecimal strings, and the calibration task is to adjust each channel’s delay so that particle arrivals all have the same digit; in our length-8 hexadecimal-string example, the arrivals are all 00000000 or 11111111 or 22222222 and so on up to FFFFFFFF. All these repeating sequences are equivalent because the model prediction is based only on relative input-channel delays so all digits being the same yield the same predicted coincidence rate.

For calibration, a difficult question concerns how many instances of channel-delay choices must be tested to enable solving of the model parameters. From Eq. (57), we know that the number of samples must scale as $n!/2$, and the exact expression is known. Consequently, to reduce the overhead required in calibrating the fermionic interferometers deterministic and on-demand single fermion sources are necessary.

VIII. DISCUSSION

In studying this problem, we have obtained some interesting, instructive results along the way, which we now summarize. Instead of simultaneity, we showed that computing exact multi-particle coincidence rates, whether bosonic or fermionic, incorporates mutual pairwise particle distinguishability, which can be expressed in terms of mode-overlap fidelity. This mode-overlap fidelity is what is controlled by channel delays between sources and interferometer, i.e., by ‘arrival time’.

Our second claim, obtained section §III B, is the exact coincidence-rate mathematical expression for any configuration of arrival times, and for any number of particles. By configuration, we refer to an array of relative arrival times for the incoming particles, with empty values \emptyset for empty input channels. In deriving the coincidence rate equations we introduce the delay matrix, which contains all information on the pairwise levels of distinguishability between particles.

As our third claim, we devised in §IV B an algorithmic method to simplify the calculation of coincidence rates, given possibly non-simultaneous arrival times. For any $s \in G_{m,n}$ our method first computes irreducible matrix representations of the submatrix $A(s)$ of a Haar-random unitary matrix U ; we then compute rates from these irreducible matrix representations. For n mutually partially distinguishable particles, our method is computationally elegant and advantageous because it is independent of the arrival times and of the numerical entries in $A(s)$, but instead leverages permutation symmetries to block diagonalize an $n! \times n!$ matrix into a sum of smaller blocks, thereby focusing the computation on the non-zero entries of the block-diagonal form. It is a clear counterpoint to the more common approach of using only permanents [74–76].

Our next claim, presented in §V A, is that we use this notion of controllable delays to formulate discretized-time coincidence rates in terms of time bins whose temporal width is the precision of channel time-delay control. Experimentally, and even philosophically, time steps are not infinitesimally tunable: a precision limit exists in practice, and this practical limit determines our coarse-graining scale to establish time bins. Throughout this paper we have referred to these time bins as discrete arrival times alluding, somewhat loosely, to controlled relative (to an arbitrary zero reference) arrival times of particles at the interferometer. Moreover, for a known set of discrete arrival times τ , we further established in §V C that specific blocks in the general sum are automatically 0 as a result of Gamas’s theorem; this leads to considerable simplifications when computing coincidence rates for a known set of discrete arrival times.

The next claim that we highlight in §VIA is our algorithm, which shows that our full exact coincidence-rate expression contains a configuration instance that requires exponentially many arithmetic operations with respect to total fermion number n . We dubbed the partition associated with this configuration instance the “witness partition”. For n even, this witness partition is $(n/2, n/2)$ and will appear in experiments when the n fermions are equally distributed over exactly two distinct time bins, or for any delay partition dominated by $(n/2, n/2)$, i.e. experimentally when at most $n/2$ fermions occupy a single time bin. The group functions or alternatively immanants associated with the witness partition needs to be evaluated and the cost of the computation scales at least exponentially with n .

For n odd, the witness partition is $((n+1)/2, (n-1)/2)$ and appears in experiments where $(n+1)/2$ fermions arrive in a single time bin, while the remaining $(n-1)/2$ fermions arrive in a single but distinct time bin; again for any delay partition dominated by $((n+1)/2, (n-1)/2)$, i.e. experimentally when at most $(n+1)/2$ fermions occupy a single time bin, the group functions or alternatively immanants for the witness partition needs to be evaluated and the cost of the computation also scales at least exponentially with n , where n is the number of mutually partially distinguishable particles.

Our sixth claim is that we calculate the probability for nonzero contribution of the above witness partition to the exact coincidence-rate calculation given uniformly random arrival times, as is expected when a calibration procedure is required. We show that this instance occurs with probability going to 1 as n increases. This is discussed in §VIB.

Finally, we have formulated the computational problem of GENFERMIONSAMPLING in Definition 18. This formulation is simple but important in that simultaneity is not intrinsic to the definition. By discarding any requirement of simultaneity, boson sampling becomes meaningfully extendable to generalized fermion sampling, and we speculate that hard-to-compute complexity can now arise in both problems.

IX. CONCLUSIONS

Our study provides a more complete understanding of the interference of partially-distinguishable particles, but the motivation for our work is stronger: our result provides an incentive to investigate the actual computational complexity of the problem defined in this work. Thus far, the focus has been on bosons but fermion sampling could extend the range of possible experiments to reach quantum advantage. Multipartite fermionic interferometry is conceivable in various settings [31] such as two-dimensional electron gases, currently restricted to two-electron interferometry. Perhaps scaling up fermion interferometry could prove to be more feasible, for many particles, than for photons, which are the currently favoured particle experimentally.

Finally, our work on the n -particle interference of bosons and fermions immediately raises questions about more exotic particles. How can our methods be applied to coincidence rates for anyons, supersymmetric particles or even strings? We do not broach these challenging topics here; rather we think that creating a common foundation for fermions and bosons creates well-posed questions that transcend these types of particles.

ACKNOWLEDGEMENTS

HdG would like to thank David Amaro Alcalá and Ari Boon for help with computer diagonalizations of some low- n cases, and Olivia Di Matteo for helpful discussions. DS thanks Andrew Berget for helpful discussions. BCS and HdG acknowledge financial support from NSERC of Canada. DS acknowledges financial support from the Ontario Graduate Scholarship.

-
- [1] Si-Hui Tan, Yvonne Y. Gao, Hubert de Guise, and Barry C. Sanders, “SU(3) quantum interferometry with single-photon input pulses,” *Phys. Rev. Lett.* **110**, 113603 (2013).
 - [2] Hubert de Guise, Si-Hui Tan, Isaac P. Poulin, and Barry C. Sanders, “Coincidence landscapes for three-channel linear optical networks,” *Phys. Rev. A* **89**, 063819 (2014).
 - [3] Max Tillmann, Si-Hui Tan, Sarah E. Stoeckl, Barry C. Sanders, Hubert de Guise, René Heilmann, Stefan Nolte, Alexander Szameit, and Philip Walther, “Generalized multiphoton quantum interference,” *Phys. Rev. X* **5**, 041015 (2015).
 - [4] Hubert de Guise and Barry C. Sanders, “Coincidence rates and permutation symmetry,” in *Quantum Communications and Quantum Imaging XV*, Vol. 10409, edited by Ronald E. Meyers, Yanhua Shih, and Keith S. Deacon, International Society for Optics and Photonics (SPIE, 2017) pp. 1–8.
 - [5] Abdullah Khalid, Dylan Spivak, Barry C. Sanders, and Hubert de Guise, “Permutational symmetries for coincidence rates in multimode multiphotonic interferometry,” *Phys. Rev. A* **97**, 063802 (2018).
 - [6] C. K. Hong, Z. Y. Ou, and L. Mandel, “Measurement of subpicosecond time intervals between two photons by interference,” *Phys. Rev. Lett.* **59**, 2044–2046 (1987).
 - [7] Yuan Liang Lim and Almut Beige, “Generalized Hong–Ou–Mandel experiments with bosons and fermions,” *New Journal of Physics* **7** (2005), 10.1088/1367-2630/7/1/155.
 - [8] Scott Aaronson and Alex Arkhipov, “The computational complexity of linear optics,” in *Proceedings of the forty-third annual ACM symposium on Theory of computing* (2011) pp. 333–342.
 - [9] Marvin Marcus and Henryk Minc, “Permanents,” *The American Mathematical Monthly* **72**, 577–591 (1965).
 - [10] Yosep Kim, Kang-Hee Hong, Joonsuk Huh, and Yoon-Ho Kim, “Experimental linear optical computing of the matrix permanent,” *Phys. Rev. A* **99**, 052308 (2019).
 - [11] A. P. Lund, A. Laing, S. Rahimi-Keshari, T. Rudolph, J. L. O’Brien, and T. C. Ralph, “Boson Sampling from a Gaussian state,” *Phys. Rev. Lett.* **113**, 100502 (2014).
 - [12] Craig S Hamilton, Regina Kruse, Linda Sansoni, Sonja Barkhofen, Christine Silberhorn, and Igor Jex, “Gaussian Boson Sampling,” *Physical review letters* **119**, 170501 (2017).
 - [13] Joonsuk Huh and Man-Hong Yung, “Vibronic Boson Sampling: Generalized Gaussian Boson Sampling for Molecular Vibronic Spectra at Finite Temperature,” *Scientific reports* **7**, 1–10 (2017).
 - [14] Juan Miguel Arrazola, Thomas R Bromley, and Patrick Rebentrost, “Quantum approximate optimization with Gaussian boson sampling,” *Physical Review A* **98**, 012322 (2018).
 - [15] Regina Kruse, Craig S Hamilton, Linda Sansoni, Sonja Barkhofen, Christine Silberhorn, and Igor Jex, “Detailed study of Gaussian boson sampling,” *Physical Review A* **100**, 032326 (2019).
 - [16] Han-Sen Zhong, Yu-Hao Deng, Jian Qin, Hui Wang, Ming-Cheng Chen, Li-Chao Peng, Yi-Han Luo, Dian Wu, Si-Qiu Gong, Hao Su, *et al.*, “Phase-Programmable Gaussian Boson Sampling Using Stimulated Squeezed Light,” *arXiv preprint arXiv:2106.15534* (2021).
 - [17] John Preskill, “Quantum computing and the entanglement frontier,” *arXiv preprint arXiv:1203.5813* (2012).
 - [18] Joonsuk Huh, Gian Giacomo Guerreschi, Borja Peropadre, Jarrod R McClean, and Alán Aspuru-Guzik, “Boson sampling for molecular vibronic spectra,” *Nature Photonics* **9**, 615–620 (2015).
 - [19] Georgios M Nikolopoulos and Thomas Brougham, “Decision and function problems based on boson sampling,” *Physical Review A* **94**, 012315 (2016).

- [20] Levon Chakhmakhchyan, Nicolas J Cerf, and Raul Garcia-Patron, “Quantum-inspired algorithm for estimating the permanent of positive semidefinite matrices,” *Physical Review A* **96**, 022329 (2017).
- [21] Georgios M Nikolopoulos, “Cryptographic one-way function based on boson sampling,” *Quantum Information Processing* **18**, 1–25 (2019).
- [22] Leonardo Banchi, Mark Fingerhuth, Tomas Babej, Christopher Ing, and Juan Miguel Arrazola, “Molecular docking with Gaussian Boson Sampling,” *Science advances* **6**, eaax1950 (2020).
- [23] T. Young, “On the theory of light and colours (the 1801 Bakerian lecture),” *Philosophical Transactions of the Royal Society of London* **92**, 12–48 (1802).
- [24] C. J. Davisson and L. H. Germer, “Reflection of Electrons by a Crystal of Nickel,” *Proc. Natl. Acad. Sci. U.S.A.* **14**, 317–322 (1928).
- [25] B. Yurke, “Interferometry with correlated fermions,” *Physica B+C* **151**, 286–290 (1988).
- [26] Roger Bach, Damian Pope, Sy-Hwang Liou, and Herman Batelaan, “Controlled double-slit electron diffraction,” *New J. Phys.* **15**, 033018 (2013).
- [27] William D. Oliver, Jungsang Kim, Robert C. Liu, and Yoshihisa Yamamoto, “Hanbury Brown and Twiss-type experiment with electrons,” *Science* **284**, 299–301 (1999), <https://science.sciencemag.org/content/284/5412/299.full.pdf>.
- [28] Roberta Ghetti and CHIC, “Fermion interferometry in ^{58}Ni -induced reactions at $E/A = 45\text{MeV}$,” *Nucl. Phys. A* **663&664**, 773c–776c (2000).
- [29] Steven E. Koonin, “Proton pictures of high-energy nuclear collisions,” *Physics Letters B* **70**, 43 – 47 (1977).
- [30] Scott Pratt and M. B. Tsang, “Viewing the liquid-gas phase transition by measuring proton correlations,” *Phys. Rev. C* **36**, 2390–2395 (1987).
- [31] Christopher Bäuerle, D Christian Glattli, Tristan Meunier, Fabien Portier, Patrice Roche, Preden Roulleau, Shintaro Takada, and Xavier Waintal, “Coherent control of single electrons: a review of current progress,” *Reports on progress in physics* **81**, 056503 (2018).
- [32] Dudley Ernest Littlewood and Archibald Read Richardson, “Group characters and algebra,” *Philosophical Transactions of the Royal Society of London. Series A, Containing Papers of a Mathematical or Physical Character* **233**, 99–141 (1934).
- [33] Carlos Gamas, “Conditions for a symmetrized decomposable tensor to be zero,” *Linear Algebra and its Applications* **109**, 83–119 (1988).
- [34] Andy Berget, “A short proof of Gamas’s theorem,” *Linear Algebra and its Applications* **430**, 791–794 (2009).
- [35] Bernard Yurke, Samuel L McCall, and John R Klauder, “SU(2) and SU(1,1) interferometers,” *Physical Review A* **33**, 4033 (1986).
- [36] GD James and A Kerber, *The Representation Theory of the Symmetric Group* (Cambridge University Press, Cambridge, 2009).
- [37] Wu-Ki Tung, *Group theory in physics: an introduction to symmetry principles, group representations, and special functions in classical and quantum physics* (World Scientific Publishing Company, 1985).
- [38] D. Lichtenberg, *Unitary Symmetry and Elementary Particles* (Elsevier, 2012).
- [39] David J Rowe and John L Wood, *Fundamentals of nuclear models: foundational models* (World Scientific, 2010).
- [40] Alexander Yong, “What is ... a Young tableau?” *Notices Am. Math. Soc.* **54**, 240–241 (2007).
- [41] Dylan Spivak, *Immanants and their applications in quantum optics*, Master’s thesis, Lakehead University, Canada (2020).
- [42] B. Kostant, “Immanant inequalities and 0-weight spaces,” *Journal of the American Mathematical Society* **8**, 181–186 (1995).
- [43] H Fearn and R Loudon, “Theory of two-photon interference,” *JOSA B* **6**, 917–927 (1989).
- [44] Charles Santori, David Fattal, Jelena Vučković, Glenn S Solomon, and Yoshihisa Yamamoto, “Indistinguishable photons from a single-photon device,” *nature* **419**, 594–597 (2002).
- [45] I. Schur, “Über endliche gruppen und hermitesche formen,” *Mathematische Zeitschrift* **1**, 184–207 (1918).
- [46] B. Kostant, “On Macdonald’s η -function formula, the Laplacian and generalized exponents,” *Advances in Mathematics* **20**, 179–212 (1976).
- [47] E Chacón and M Moshinsky, “Representations of finite U_3 transformations,” *Physics Letters* **23**, 567–569 (1966).
- [48] D. J. Rowe, B. C. Sanders, and H. de Guise, “Representations of the Weyl group and Wigner functions for SU(3),” *Journal of Mathematical Physics* **40**, 3604–3615 (1999).
- [49] E. P. Wigner, “Group theory,” (1959).
- [50] Arne Alex, Matthias Kalus, Alan Huckleberry, and Jan von Delft, “A numerical algorithm for the explicit calculation of SU(n) and SL(n,C) Clebsch–Gordan coefficients,” *Journal of Mathematical Physics* **52**, 023507 (2011).
- [51] Asim Orhan Barut and Ryszard Raczka, *Theory of group representations and applications* (World Scientific, 1986).
- [52] IM Gelfand and ML Tsetlin, “Matrix elements for the unitary groups,” in *Dokl. Akad. Nauk U.S.S.R.*, Vol. 71 (1950) pp. 825–828.
- [53] Jin-Quan Chen, Jialun Ping, and Fan Wang, *Group Representation Theory for Physicists*, Vol. 7 (World Scientific, 1989).
- [54] M Jerrum, A Sinclair, and E Vigoda, “A polynomial-time approximation algorithm for the permanent of a matrix with non-negative entries,” *Journal of the ACM* **51**, 671–697 (2004).
- [55] J. A. Dias da Silva, “On the μ -colorings of a matroid,” *Linear and Multilinear Algebra* **27**, 25–32 (1990).
- [56] P. Bürgisser, “The computational complexity to evaluate representations of general linear groups,” *SIAM Journal on Computing* **30**, 1010–1022 (2000).
- [57] Donald Ervin Knuth, *The Art of Computer Programming*, 3rd ed., Vol. 1 (Addison Wesley Longman, Reading, MA, 1997).
- [58] Michael A. Nielsen and Isaac L. Chuang, *Quantum Computation and Quantum Information: 10th Anniversary Edition*, 10th ed. (Cambridge University Press, USA, 2011).
- [59] Barry C Sanders, *How to Build a Quantum Computer*, 2399–2891 (IOP Publishing, 2017).
- [60] Bettina Heim, Troels F. Rønnow, Sergei V. Isakov, and Matthias Troyer, “Quantum versus classical annealing of Ising spin glasses,” *Science* **348**, 215–217 (2015).
- [61] Daniel J. Brod, Ernesto F. Galvão, Andrea Crespi, Roberto Osellame, Nicolò Spagnolo, and Fabio Sciarrino, “Photonic implementation of boson sampling: a review,” *Advanced Photonics* **1**, 1–14 (2019).
- [62] Peter P. Rohde and Timothy C. Ralph, “Error tolerance of the BosonSampling model for linear optics quantum computing,” *Phys. Rev. A* **85**, 022332 (2012).

- [63] Scott Aaronson and Alex Arkhipov, “BosonSampling is far from uniform,” arXiv preprint arXiv:1309.7460 (2013).
- [64] Terry Rudolph, “Why I am optimistic about the silicon-photon route to quantum computing,” *APL Photonics* **2**, 030901 (2017).
- [65] Michał Oszmaniec, Ninnat Dangniam, Mauro ES Morales, and Zoltán Zimborás, “Fermion Sampling: a robust quantum computational advantage scheme using fermionic linear optics and magic input states,” arXiv preprint arXiv:2012.15825 (2020).
- [66] Barbara M. Terhal and David P. DiVincenzo, “Classical simulation of noninteracting-fermion quantum circuits,” *Phys. Rev. A* **65**, 032325 (2002).
- [67] David P. DiVincenzo and Barbara M. Terhal, “Fermionic linear optics revisited,” *Found. Phys.* **35**, 1967–1984 (2005).
- [68] Peter Heyfron, “Immanant dominance orderings for hook partitions,” *Linear and Multilinear Algebra* **24**, 65–78 (1988).
- [69] Peter Heyfron, “Some inequalities concerning immanants,” in *Mathematical Proceedings of the Cambridge Philosophical Society*, Vol. 109 (Cambridge University Press, 1991) pp. 15–30.
- [70] Thomas H Pate, “Partitions, irreducible characters, and inequalities for generalized matrix functions,” *Transactions of the American Mathematical Society* **325**, 875–894 (1991).
- [71] John R Stembridge, “Immanants of totally positive matrices are nonnegative,” *Bull. London Math. Soc* **23**, 422–428 (1991).
- [72] Felix Huber and Hans Maassen, “Matrix forms of immanant inequalities,” arXiv preprint arXiv:2103.04317 (2021).
- [73] Wojciech Górecki, Rafał Demkowicz-Dobrzański, Howard M. Wiseman, and Dominic W. Berry, “ π -corrected Heisenberg limit,” *Phys. Rev. Lett.* **124**, 030501 (2020).
- [74] VS Shchesnovich, “Partial indistinguishability theory for multiphoton experiments in multiport devices,” *Physical Review A* **91**, 013844 (2015).
- [75] Vincenzo Tamma and Simon Laibacher, “Boson sampling with non-identical single photons,” *Journal of Modern Optics* **63**, 41–45 (2016).
- [76] Malte C Tichy, “Sampling of partially distinguishable bosons and the relation to the multidimensional permanent,” *Physical Review A* **91**, 022316 (2015).